Fig. 1 a Western blot analysis of collagen type IV, fibronectin, TIMP-1, MMP-2 and MMP-9 proteins in PnMECs and peripheral nerve pericytes. Fibronectin, collagen type IV, TIMP-1, MMP-2 and MMP-9 bands corresponded to single bands at 190, 25, 38, and 92 kDa, respectively. Bands corresponding to collagen type IV and TIMP-1 were not detected in PnMECs, although the fibronectin, MMP-2 and MMP-9 proteins were

visualised. b–d The bar graph reflects the combined densitometry data from five independent experiments (mean±SEM, $n=5$). The production of fibronectin (b) and pro-MMP-2 (c) in peripheral nerve pericytes was significantly higher than in PnMECs, whereas production of pro-MMP-9 protein (d) did not show a significant difference between these two cell lines. $**p<0.01$

TIMP-1 bands were not detected, the fibronectin, MMP-2, and MMP-9 proteins were produced in PnMECs (Fig. 1a). Interestingly, the production of fibronectin (Fig. 1b) and MMP-2 (Fig. 1c) proteins in the peripheral nerve pericytes was significantly higher than those in PnMECs ($p<0.01$), whereas production of MMP-9 protein production did not show a significant difference between these two cells (Fig. 1d).

Effect of AGEs on the production of basement-membrane-related molecules in peripheral nerve pericytes To identify the possible mechanism responsible for the basement membrane hypertrophy of the BNB after exposure to AGEs, we also examined the changes in the production of fibronectin, collagen type IV, TIMP-1, MMP-2 and MMP-9 proteins in peripheral nerve pericytes after AGE exposure (100, 200 μg/ml; Fig. 2a). The production of fibronectin and collagen type IV protein in peripheral nerve pericytes significantly increased in a dose-dependent manner after exposure to AGEs ($p<0.01$; Table 1). The TIMP-1 protein production in peripheral nerve pericytes was also significantly increased after application of AGEs; however, the production of active MMP-9 (act-MMP-9) was decreased by treatment with 200 μg/ml AGE (Table 1). The level of the receptor of AGE (RAGE) in peripheral nerve pericytes was observed to increase significantly after incubation with AGEs in a dose-dependent manner (Table 1). We previously reported that our peripheral nerve pericytes released several growth factors, including VEGF, TGF-β and bFGF, to maintain peripheral nerve homeostasis at the BNB [15]. We also quantified the change of these growth factors in

peripheral nerve pericytes after incubation with AGEs (100 and 200 μg/ml) by a western blot analysis (Fig. 2b). The production of VEGF and TGF-β protein in peripheral nerve pericytes was significantly increased by treatment with AGEs, although there was no change in the bFGF protein production after AGE exposure (Table 1).

Contribution of TGF-β1 and VEGF to the induction of basement-membrane-related molecules after AGE exposure TGF-β1 and VEGF are known to be major mediators of the early and late vascular changes in diabetic microangiopathy. To investigate the effect of TGF-β1 and VEGF on the production of basement-membrane-related molecules at the BNB, we also quantified the changes in the production of fibronectin, collagen type IV, TIMP-1, MMP-2 and MMP-9 in peripheral nerve pericytes after incubation with TGF-β1 (10 ng/ml) and VEGF (10 ng/ml) by western blot analysis (Fig. 3). Fibronectin and collagen type IV in peripheral nerve pericytes significantly increased after exposure to TGF-β1 or VEGF ($p<0.01$; Table 2). The promatrix metalloproteinase (pro-MMP-9) protein in peripheral nerve pericytes was also upregulated ($p<0.01$) after application of TGF-β1 or VEGF (Table 2). To clarify the individual contributions of VEGF and TGF-β1 to the increase in basement-membrane thickness after exposure to AGEs, the activities of VEGF and TGF-β were neutralised using an anti-VEGF and anti-TGF-β antibody. The production of fibronectin and collagen type IV protein in peripheral nerve pericytes was decreased after incubation with AGEs pretreated with the anti-TGF-β

Fig. 2 a The changes in collagen type IV, fibronectin, TIMP-1, MMP-2 and MMP-9 production in peripheral nerve pericytes after treatment with the two AGE concentrations (100 and 200 μg/ml). The production of fibronectin, collagen type IV, TIMP-1 and RAGE in peripheral nerve pericytes was significantly increased after treatment with AGEs in a dose-dependent manner. The level of act-MMP-9 proteins in peripheral nerve pericytes was significantly reduced, whereas act-MMP-2 protein did not show a significant difference following AGE treatment. **b** The changes in TGF-β, VEGF and bFGF production in peripheral nerve pericytes treated with AGEs. The production of TGF-β and VEGF in peripheral nerve pericytes was significantly increased after treatment with AGEs, whereas bFGF production was not affected following AGE treatment. Control, conditioned medium of unmodified BSA; AGE, condition medium of AGEs–BSA
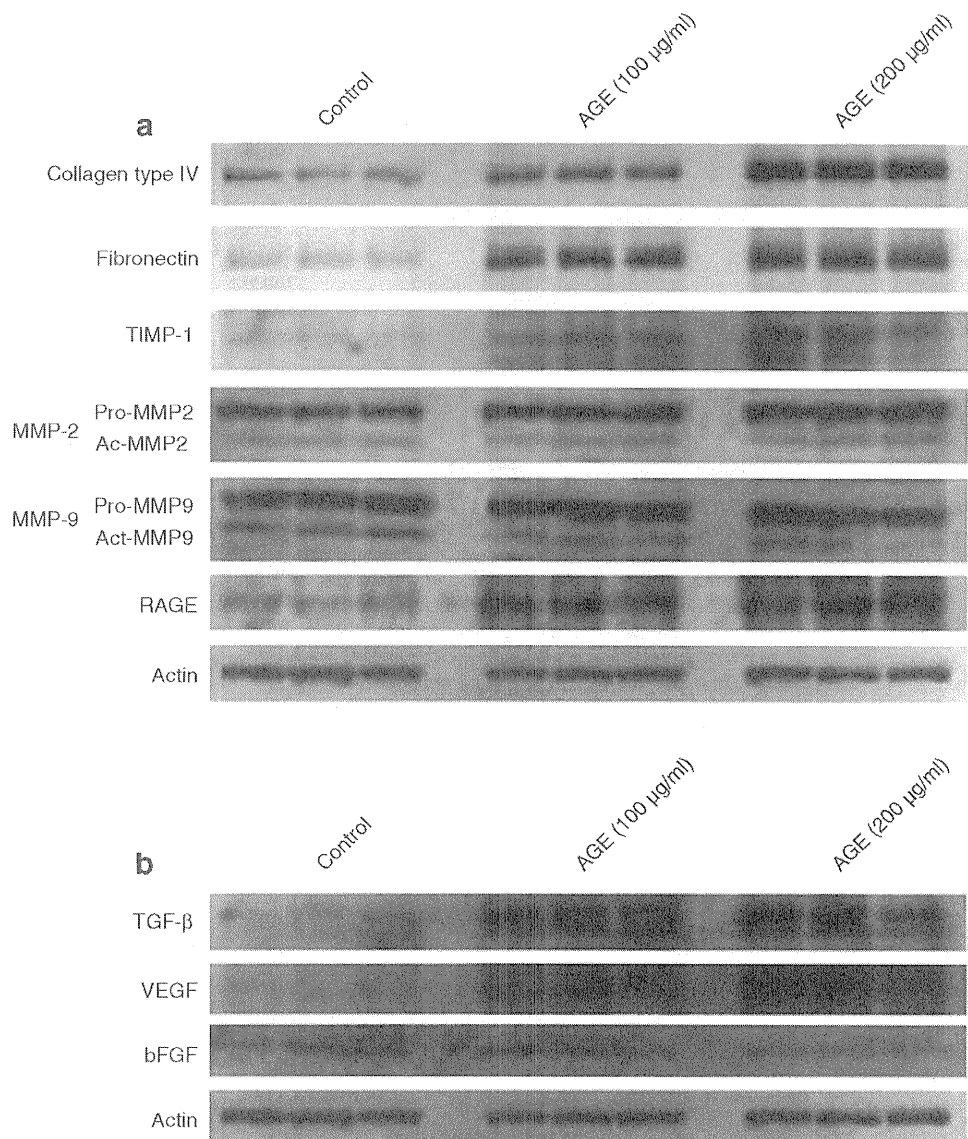
(Fig. 4a–c) or VEGF (Fig. 4d–f) antibody, as determined by a western blot analysis.

Effect of AGEs on the production of tight junctional molecules by PnMECs, and the contribution of VEGF to the induction of claudin-5 after AGE exposure To determine the effect of AGEs on the barrier function of the BNB, we also examined the changes in claudin-5 production by PnMECs after exposure to AGE (100 μg/ml) by a western blot analysis (Fig. 5a). Whereas the claudin-5 production in PnMECs was significantly reduced (Fig. 5b), VEGF production was significantly increased after incubation with AGEs (Fig. 5c). The TEER value of PnMECs did not change after incubation with AGEs (Fig. 5h). To clarify

the contribution of VEGF to the reduction of claudin-5 in PnMECs, a neutralising anti-VEGF antibody was used. Relative quantification with real-time RT-PCR revealed that the percentage of increase in the claudin-5 (*CLDN5*) mRNA expression was 48% after incubation with AGEs pretreated using the anti-VEGF antibody (Fig. 5e). In addition, we quantified claudin-5 protein in PnMECs after incubation with the anti-VEGF neutralising antibody (Fig. 5f). Production of claudin-5 protein was increased after pre-incubation with the anti-VEGF neutralising antibody (Fig. 5g). The TEER value of PnMECs was also significantly increased after exposure to AGEs in cells pretreated with the anti-VEGF neutralising antibody (Fig. 5h). RAGE production in PnMECs
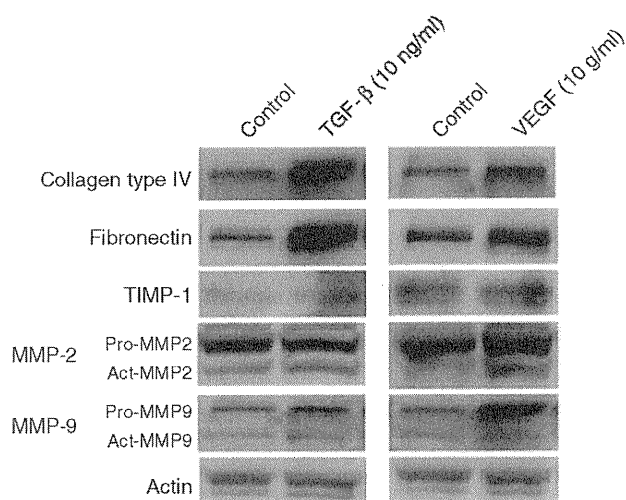
Fig. 3 The effect of VEGF (10 ng/ml) and TGF-β (10 ng/ml) on production of collagen type IV, fibronectin, TIMP-1, MMP-2, and MMP-9 proteins in peripheral nerve pericytes. The production of collagen type IV and fibronectin in peripheral nerve pericytes was significantly increased after treatment with TGF-β. The pro-MMP-9 proteins in peripheral nerve pericytes were upregulated after incubation with TGF-β, although TIMP-1 production was not affected. The production of collagen type IV and fibronectin in peripheral nerve pericytes was significantly increased after treatment with VEGF. The pro-MMP-9 proteins in peripheral nerve pericytes were upregulated after incubation with VEGF, although TIMP-1 production was not affected

was significantly induced after the application of AGEs (Fig. 5d).

Discussion

In this study, we examined the importance of the cells comprising the BNB in the formation or maintenance of the basement membrane. We have successfully established PnMEC and peripheral nerve pericyte cell lines of human origin [15, 16]. Therefore, our in vitro BNB model is considered suitable for the analysis of the production of basement-membrane-related molecules, because it is difficult to identify cells that synthesise these molecules in vivo. Our study demonstrated that fibronectin, collagen type IV, MMP-2 and TIMP-1 are mainly synthesised by peripheral nerve pericytes, confirming that the maintenance of the basement membrane components is regulated primarily by peripheral nerve pericytes at the BNB. The basement membrane of the BBB is constructed from ECM-related molecules, including collagen type IV and fibronectin, and is regulated by TIMP-1, which inhibits MMPs [8]. Several studies suggest that astrocytes and brain pericytes synthesise fibronectin and collagen type IV, and these cells secrete

MMP-2 and MMP-9 to maintain basement membrane turnover [11, 17]. Our study verified that peripheral nerve pericytes, which are the only cells in the endoneurial microvessels other than PnMECs, might be the key cells with regard to the maintenance of the basement membrane at the BNB.

The breakdown of the BNB is considered to be a key step in diabetic neuropathy [5, 6]. Investigations of biopsied nerves with mild to severe diabetic neuropathy showed structural changes in the microvasculature in the endoneurium, including an increase in the basement membrane thickness, pericyte degeneration and endothelial hyperplasia [6]. Although basement membrane hypertrophy at the BNB is one of the cardinal pathogenic features of diabetic neuropathy [6], its pathogenesis remains unclear. TGF-β1 is generally accepted to be the main pro-fibrotic factor in diabetic nephropathy [13]. Several lines of experimental and clinical evidence support a major role for TGF-β1 in the development of glomerulosclerosis and interstitial fibrosis in diabetic nephropathy [18, 19]. In another study, inhibition of TGF-β1 with neutralising antibodies prevented the glomerular enlargement and the excess matrix production by reducing collagen type IV and fibronectin [20, 21]. Conversely, VEGF is also known to be another mediator of the early and late vascular changes in diabetic nephropathy and retinopathy. Several studies have suggested that VEGF signalling may affect renal matrix accumulation, because inhibition of VEGF with neutralising antibodies attenuates the increase in glomerular basement membrane thickness and mesangial matrix expansion in diabetic nephropathy [13, 22]. Furthermore, recent evidence has shown that VEGF may contribute to the breakdown of the BRB during diabetic retinopathy because

Table 2 Effect of TGF-β and VEGF on production of basement-membrane-related molecules in peripheral nerve pericytes

Protein	Ratio of target protein production (protein:actin)	
	TGF-β	VEGF
Collagen type IV	4.49±0.15**	1.94±0.20**
Fibronectin	3.60±0.18**	1.92±0.15**
TIMP-1	1.23±0.14	1.10±0.14
Pro-MMP-9	1.84±0.13**	3.22±0.23**
Act-MMP-9	1.28±0.14	1.38±0.17
Pro-MMP-2	0.95±0.14	1.34±0.25
Act-MMP-2	1.43±0.32	1.32±0.14

Data shown are means±SEM ($n=5$)

Each value reflects the combined densitometry data from five independent experiments and is shown as a fold increase above control
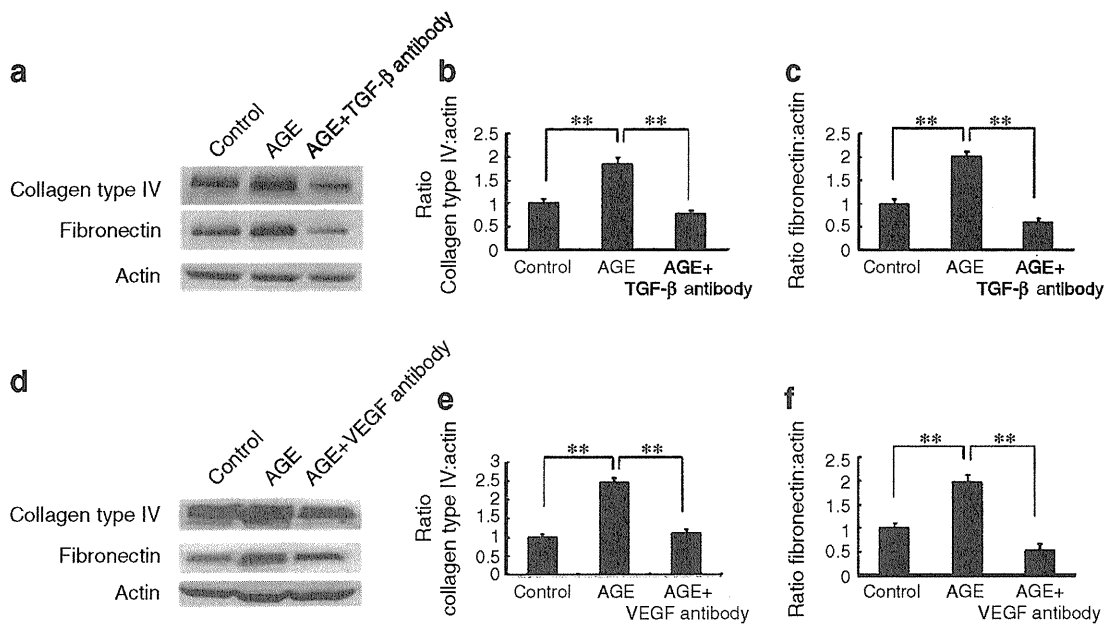
**$p<0.01$ compared with control

a

Control / AGE / AGE+TGF-β antibody

Collagen type IV
Fibronectin
Actin

b

Ratio Collagen type IV:actin

2.5
2
1.5
1
0.5
0

Control   AGE   AGE+
TGF-β antibody

** **

c

Ratio fibronectin:actin

2.5
2
1.5
1
0.5
0

Control   AGE   AGE+
TGF-β antibody

** **

d

Control / AGE / AGE+VEGF antibody

Collagen type IV
Fibronectin
Actin

e

Ratio collagen type IV:actin

3
2.5
2
1.5
1
0.5
0

Control   AGE   AGE+
VEGF antibody

** **

f

Ratio fibronectin:actin

2.5
2
1.5
1
0.5
0

Control   AGE   AGE+
VEGF antibody

** **

Fig. 4 The effects of anti-TGF-β and anti-VEGF neutralising antibodies on the collagen type IV and fibronectin induction by treatment with AGEs. The peripheral nerve pericytes were cultured with AGEs or AGEs pre-treated with anti-TGF-β or anti-VEGF antibody for 24 h. **a** The change in the production of collagen type IV and fibronectin protein in PnMECs after treatment with anti-TGF-β neutralising antibody using a western blot analysis. **b** Collagen type IV and (**c**) fibronectin proteins were inhibited after pretreatment with anti-TGF-β neutralising antibody. **d** The change in the production of collagen type IV and fibronectin protein in PnMECs after treatment with anti-VEGF neutralising antibody using a western blot analysis. Production of (**e**) collagen type IV and (**f**) fibronectin was inhibited after pretreatment with anti-VEGF neutralising antibody. Each bar graph reflects the combined densitometry data from five independent experiments (mean±SEM, $n=5$). Control, conditioned medium of unmodified BSA; AGEs, conditioned medium of AGEs–BSA; AGE+VEGF antibody, conditioned medium of AGEs–BSA pre-treated with VEGF neutralising antibody; AGE+TGF-β antibody, conditioned medium of AGE–BSA pre-treated with TGF-β neutralising antibody; **$p<0.01$

of the beneficial effects of anti-VEGF agents in the reduction of retinal vascular permeability [23]. We therefore hypothesised that TGF-β and VEGF signalling may contribute to the induction of basement membrane hypertrophy and disruption of the BNB. Our study demonstrated that the production of fibronectin and collagen type IV by peripheral nerve pericytes significantly increased after exposure to TGF-β or VEGF, and that the amount of pro-MMP-9 significantly increased. These results indicate that TGF-β and VEGF might directly stimulate the production of fibronectin and collagen type IV in peripheral nerve pericytes, and that the induction of pro-MMP-9 might then occur secondary to these signals, thus leading to degradation of the increased fibronectin or collagen type IV in order to maintain ECM turnover.

AGEs are the late products of non-enzymatic glycation, and their accumulation on proteins in the microvasculature appears to be a key factor in the development of neuropathy [24]. AGEs accumulate in the vessel walls and have been implicated in both the macrovascular and microvascular complications of diabetes [12]. The accumulation of AGEs in both the peripheral nerves of human diabetic patients and

in the experimental diabetic animals was observed in vascular endothelial cells, pericytes, and the basement membrane, as well as in axons and Schwann cells, thus resulting in an impaired nerve function and characteristic pathological alterations [24, 25]. Several lines of evidences suggest that AGEs induce basement-membrane thickening in diabetic nephropathy and retinopathy [13, 26]. However, the molecular mechanism underlying this process is unclear in diabetic neuropathy. Our study demonstrates that the production of collagen type IV and fibronectin in peripheral nerve pericytes was significantly increased after exposure to AGEs. These results thus indicate that AGEs directly induce basement membrane hypertrophy at the BNB.

Several other studies suggest that an imbalance between MMPs and TIMPs may cause basement membrane hypertrophy through inhibition of ECM degradation [9, 13]. Our results demonstrated that induction of TIMP-1 and reduction of MMP-9 in peripheral nerve pericytes was observed after application of AGEs, thus suggesting that AGEs inhibit ECM degradation at the BNB. Furthermore, our study also demonstrated that the production of VEGF and TGF-β secreted from peripheral nerve pericytes was
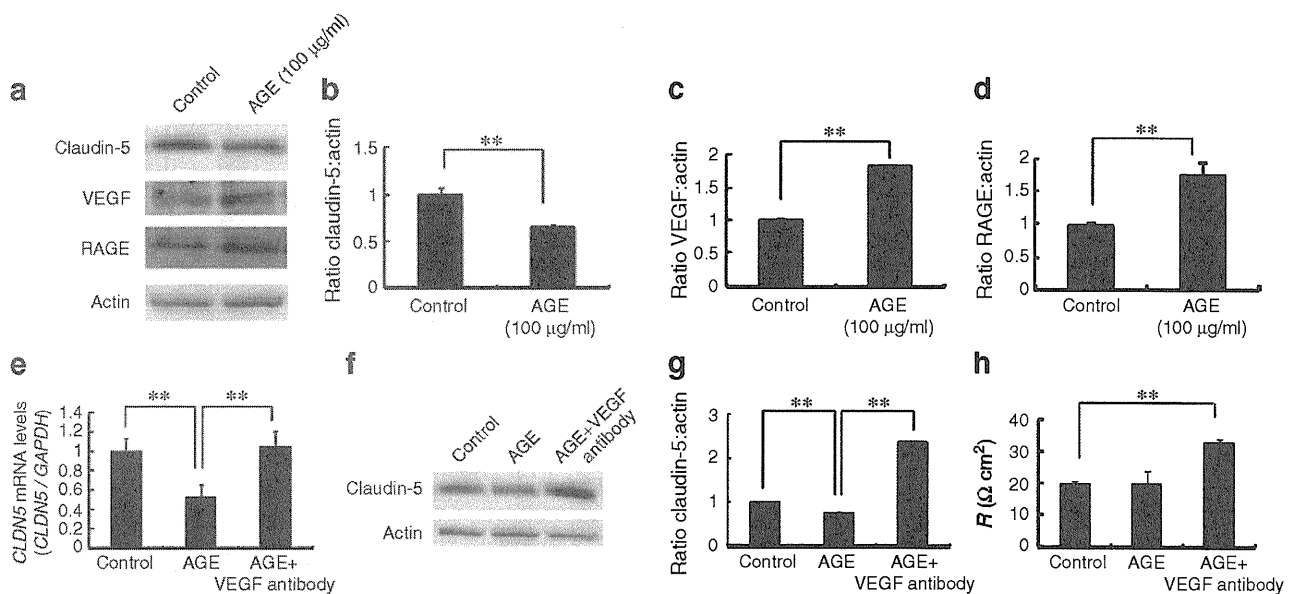
Fig. 5 a The changes in claudin-5, VEGF and RAGE production in peripheral nerve pericytes after treatment with AGEs (100 μg/ml) using western blot analysis. b Claudin-5 in PnMECs was significantly decreased after treatment with AGE. VEGF (c) and (d) RAGE production was significantly increased after incubation with AGE. e The effect of anti-VEGF neutralising antibody on the CLDN5 induction by AGE treatment. The PnMECs were cultured with AGEs or AGEs pre-treated with anti-VEGF antibody for 24 h. The level of CLDN5 mRNA in PnMECs was assayed by real-time RT-PCR and expressed as the ratio of the target gene/GAPDH. The CLDN5 mRNA was upregulated by 48% following exposure to AGEs pretreated with anti-VEGF antibody as compared with AGEs only. f The change in the production of claudin-5 protein in PnMECs after treatment with anti-VEGF neutralising antibody using western blot analysis. g Claudin-5 protein was increased after pretreatment with anti-VEGF neutralising antibody. h The TEER value of PnMECs was also significantly increased after treatment with AGEs pretreated with anti-VEGF neutralising antibody. Each bar graph reflects the combined densitometry data from five independent experiments (mean±SEM, $n=5$). Control, conditioned medium of unmodified BSA; AGEs, conditioned medium of AGEs–BSA; AGE+VEGF antibody, a conditioned medium of AGE–BSA pre-treated with VEGF neutralising antibody. **$p<0.01$

increased after incubation with AGEs. The experimental inhibition studies using anti-VEGF or TGF-β neutralising antibodies in peripheral nerve pericytes also revealed that VEGF and TGF-β were primarily responsible for the upregulation of fibronectin and collagen type IV. These results indicate that AGEs induce basement membrane hypertrophy and disrupt the BNB by increasing the production of secreted VEGF and TGF-β by pericytes under diabetic conditions.

The breakdown of the BRB occurs in patients with diabetic retinopathy [27]. Several studies have suggested that AGEs induce vasopermeability of the retina by increasing VEGF production [14, 23, 28–31] and disrupt the BRB by decreasing tight junction proteins, such as occludin and ZO-1 [32]. However, the role of AGEs in diabetic neuropathy remains unclear. In this study, we examined whether AGEs could alter the integrity of the tight junction in endothelial cells during diabetic neuropathy. Claudin-5 is known to be a major component of tight junctions, and the production of claudin-5 is important for tight junction maintenance in the mature BBB [33]. Our results demonstrate that claudin-5 in PnMECs was

decreased after exposure to AGEs. In contrast, the production of VEGF in PnMECs was increased after incubation with AGEs, and our inhibition studies using an anti-VEGF neutralising antibody also revealed that VEGF was primarily responsible for the downregulation of claudin-5. These results indicate that AGEs reduce the production of claudin-5 in PnMECs by increasing the secretion of VEGF secreted by the PnMECs themselves.

Our findings show that the production of RAGE was significantly increased in peripheral nerve pericytes and PnMECs after exposure to AGEs. RAGE is a 35 kDa polypeptide of the Ig superfamily that plays a critical role in the development of diabetic vascular complications [34, 35]. RAGE is present in minimal quantities in the normal endothelial cells and pericytes of the BNB, but is upregulated in a positive-feedback manner when AGE ligands accumulate [24, 36]. These activities may induce inflammatory responses, leading to aggravation of diabetic vascular complications [36]. RAGE has also been reported to activate transcription factor nuclear factor κB cells (NF-κB), thus leading to increase production of the cytokines including TNF-α [34, 35]. Several studies have demon-

strated that NF-κB activation may induce VEGF and TGF-β production [37, 38]. The activation of RAGE in PnMECs and peripheral nerve pericytes after exposure to AGEs may thus induce the production of VEGF and TGF-β through NF-κB signalling. The prevention or decrease of glycation and glycation-induced tissue damage could be possible therapeutic strategies for the treatment of diabetic neuropathy [39, 40]. Recent clinical studies have shown that AGE breakers, including ALT-711 and alagebrium, may be able to decrease the adverse vascular effects of glycation with few side effects [41–43], although no benefits have been demonstrated in the area of neuropathy. The inhibition of pathological responses mediated by AGEs may have therapeutic potential for diabetic neuropathy, although the RAGE-mediated molecular mechanisms need to be explored in further studies.

In conclusion, we have herein demonstrated that pericytes are the main regulators involved in the maintenance of the basement membrane at the BNB, and that AGEs induce basement membrane hypertrophy and disrupt the BNB by increasing the secretion of VEGF and TGF-β released by pericytes and the secretion of VEGF secreted by PnMECs under diabetic conditions. Further research is necessary because obtaining a better understanding of the molecular mechanisms by which AGEs induce BNB breakdown is expected to provide new targets for the treatment and prevention of diabetic neuropathy.

References

1. Abbott NJ, Rönnbäck L, Hansson E (2006) Astrocyte-endothelial interactions at the blood-brain barrier. Nat Rev Neurosci 7:41–53
2. Poduslo JF, Curran GL, Berg CT (1994) Macromolecular permeability across the blood–nerve and blood–brain barriers. Proc Natl Acad Sci USA 91:5705–5709
3. Sano Y, Shimizu F, Nakayama H, Abe M, Maeda T, Ohtsuki S, Terasaki T, Obinata M, Ueda M, Takahashi R, Kanda T (2007) Endothelial cells constituting blood-nerve barrier have highly specialized characteristics as barrier-forming cells. Cell Struct Funct 32:139–147
4. Vinik AI, Mehrabyan A (2004) Diabetic neuropathies. Med Clin North Am 88:947–999
5. Cameron NE, Eaton SE, Cotter MA, Tesfaye S (2001) Vascular factors and metabolic interactions in the pathogenesis of diabetic neuropathy. Diabetologia 44:1973–1988
6. Giannini C, Dyck PJ (1995) Basement membrane reduplication and pericyte degeneration precede development of diabetic polyneuropathy and are associated with its severity. Ann Neurol 37:498–504
7. Grant DS, Kleinman HK (1997) Regulation of capillary formation by laminin and other components of the extracellular matrix. EXS 79:317–333
8. Tilling T, Engelbertz C, Decker S, Korte D, Hüwel S, Galla HJ (2002) Expression and adhesive properties of basement membrane proteins in cerebral capillary endothelial cell cultures. Cell Tissue Res 310:19–29
9. Davis GE, Senger DR (2005) Endothelial extracellular matrix: biosynthesis, remodeling, and functions during vascular morphogenesis and neovessel stabilization. Circ Res 97:1093–1107
10. Jiang B, Liou GI, Behzadian MA, Caldwell RB (1994) Astrocytes modulate retinal vasculogenesis: effects on fibronectin expression. J Cell Sci 107:2499–2508
11. Kose N, Asashima T, Muta M, Iizasa H, Sai Y, Terasaki T, Nakashima E (2007) Altered expression of basement membrane-related molecules in rat brain pericyte, endothelial, and astrocyte cell lines after transforming growth factor-beta1 treatment. Drug Metab Pharmacokinet 22:255–266
12. Goldin A, Beckman JA, Schmidt AM, Creager MA (2006) Advanced glycation end products: sparking the development of diabetic vascular injury. Circulation 114:597–605
13. Ban CR, Twigg SM (2008) Fibrosis in diabetes complications: pathogenic mechanisms and circulating and urinary markers. Vasc Health Risk Manag 4:575–596
14. Canning P, Glenn JV, Hsu DK, Liu FT, Gardiner TA, Stitt AW (2007) Inhibition of advanced glycation and absence of galectin-3 prevent blood-retinal barrier dysfunction during short-term diabetes. Exp Diabetes Res: 51837
15. Shimizu F, Sano Y, Abe MA, Maeda T, Ohtsuki S, Terasaki T, Obinata M, Kanda T (2011) Peripheral nerve pericytes modify the blood-nerve barrier function and tight junctional molecules through the secretion of various soluble factors. J Cell Physiol 226:255–266
16. Shimizu F, Sano Y, Maeda T, Abe MA, Nakayama H, Takahashi R, Ueda M, Ohtsuki S, Terasaki T, Obinata M, Kanda T (2008) Peripheral nerve pericytes originating from the blood-nerve barrier expresses tight junctional molecules and transporters as barrier-forming cells. J Cell Physiol 217:388–399
17. Muir EM, Adcock KH, Morgenstern DA, Clayton R, von Stillfried N, Rhodes K, Ellis C, Fawcett JW, Rogers JH (2002) Matrix metalloproteases and their inhibitors are produced by overlapping populations of activated astrocytes. Brain Res Mol Brain Res 100:103–117
18. Ziyadeh FN, Han DC, Cohen JA, Guo J, Cohen MP (1998) Glycated albumin stimulates fibronectin gene expression in glomerular mesangial cells: involvement of the transforming growth factor-beta system. Kidney Int 53:631–638
19. Sharma K, Ziyadeh FN (1995) Hyperglycemia and diabetic kidney disease. The case for transforming growth factor-beta as a key mediator. Diabetes 44:1139–1146
20. Sharma K, Jin Y, Guo J, Ziyadeh FN (1996) Neutralization of TGF-beta by anti-TGF-beta antibody attenuates kidney hypertrophy and the enhanced extracellular matrix gene expression in STZ-induced diabetic mice. Diabetes 45:522–530
21. Ziyadeh FN, Hoffman BB, Han DC, Iglesias-De La Cruz MC, Hong SW, Isono M, Chen S, McGowan TA, Sharma K (2000) Long-term prevention of renal insufficiency, excess matrix gene expression, and glomerular mesangial matrix expansion by treatment with monoclonal antitransforming growth factor-beta antibody in db/db diabetic mice. Proc Natl Acad Sci USA 97:8015–8020
22. Sung SH, Ziyadeh FN, Wang A, Pyagay PE, Kanwar YS, Chen S (2006) Blockade of vascular endothelial growth factor signaling ameliorates diabetic albuminuria in mice. J Am Soc Nephrol 17:3093–3104

23. Penn JS, Madan A, Caldwell RB, Bartoli M, Caldwell RW, Hartnett ME (2008) Vascular endothelial growth factor in eye disease. Prog Retin Eye Res 27:331–371

24. Wada R, Yagihashi S (2005) Role of advanced glycation end products and their receptors in development of diabetic neuropathy. Ann NY Acad Sci 1043:598–604

25. Sugimoto K, Nishizawa Y, Horiuchi S, Yagihashi S (1997) Localization in human diabetic peripheral nerve of N(epsilon)-carboxymethyllysine-protein adducts, an advanced glycation end-product. Diabetologia 40:1380–1387

26. Tsilibary EC (2003) Microvascular basement membranes in diabetes mellitus. J Pathol 200:537–546

27. Khan ZA, Chakrabarti S (2007) Cellular signaling and potential new treatment targets in diabetic retinopathy. Exp Diabetes Res. 31867

28. Stitt AW, Bhaduri T, McMullen CB, Gardiner TA, Archer DB (2000) Advanced glycation end products induce blood-retinal barrier dysfunction in normoglycemic rats. Mol Cell Biol Res Commun 3:380–388

29. Lu M, Kuroki M, Amano S, Tolentino M, Keough K, Kim I, Bucala R, Adamis AP (1998) Advanced glycation end products increase retinal vascular endothelial growth factor expression. J Clin Invest 101:1219–1224

30. Yamagishi S, Yonekura H, Yamamoto Y, Katsuno K, Sato F, Mita I, Ooka H, Satozawa N, Kawakami T, Nomura M, Yamamoto H (1997) Advanced glycation end products-driven angiogenesis in vitro. Induction of the growth and tube formation of human microvascular endothelial cells through autocrine vascular endothelial growth factor. J Biol Chem 272:8723–8730

31. McFarlane S, Glenn JV, Lichanska AM, Simpson DA, Stitt AW (2005) Characterisation of the advanced glycation endproduct receptor complex in the retinal pigment epithelium. Br J Ophthalmol 89:107–112

32. Sheikpranbabu S, Kalishwaralal K, Lee KJ, Vaidyanathan R, Eom SH, Gurunathan S (2010) The inhibition of advanced glycation end-products-induced retinal vascular permeability by silver nanoparticles. Biomaterials 31:2260–2271

33. Nitta T, Hata M, Gotoh S, Seo Y, Sasaki H, Hashimoto N, Furuse M, Tsukita S (2003) Size-selective loosening of the blood-brain barrier in claudin-5-deficient mice. J Cell Biol 161:653–660

34. Farmer DG, Kennedy S (2009) RAGE, vascular tone and vascular disease. Pharmacol Ther 124:185–194

35. Yonekura H, Yamamoto Y, Sakurai S, Watanabe T, Yamamoto H (2005) Roles of the receptor for advanced glycation endproducts in diabetes-induced vascular injury. J Pharmacol Sci 97:305–311

36. Lukic IK, Humpert PM, Nawroth PP, Bierhaus A (2008) The RAGE pathway: activation and perpetuation in the pathogenesis of diabetic neuropathy. Ann NY Acad Sci 1126:76–80

37. Djordjević G, Matusan-Ilijas K, Sinozić E, Damante G, Fabbro D, Grahovac B, Lucin K, Jonjić N (2008) Relationship between vascular endothelial growth factor and nuclear factor-kappaB in renal cell tumors. Croat Med J 49:608–617

38. Saile B, Matthes N, El Armouche H, Neubauer K, Ramadori G (2001) The bcl, NFkappaB and p53/p21WAF1 systems are involved in spontaneous apoptosis and in the anti-apoptotic effect of TGF-beta or TNF-alpha on activated hepatic stellate cells. Eur J Cell Biol 80:554–561

39. Huijberts MS, Schaper NC, Schalkwijk CG (2008) Advanced glycation end products and diabetic foot disease. Diabetes Metab Res Rev 24:S19–S24

40. Monnier VM (2003) Intervention against the Maillard reaction in vivo. Arch Biochem Biophys 419:1–15

41. Kass DA, Shapiro EP, Kawaguchi M, Capriotti AR, Scuteri A, deGroof RC, Lakatta EG (2001) Improved arterial compliance by a novel advanced glycation end-product crosslink breaker. Circulation 104:1464–1470

42. Little WC, Zile MR, Kitzman DW, Hundley WG, O'Brien TX, Degroof RC (2005) The effect of alagebrium chloride (ALT-711), a novel glucose cross-link breaker, in the treatment of elderly patients with diastolic heart failure. J Card Fail 11:191–195

43. Zieman SJ, Melenovsky V, Clattenburg L, Corretti MC, Capriotti A, Gerstenblith G, Kass DA (2007) Advanced glycation endproduct crosslink breaker (alagebrium) improves endothelial function in patients with isolated systolic hypertension. J Hypertens 25:577–583

Peripheral Nerve Pericytes Modify the Blood–Nerve Barrier Function and Tight Junctional Molecules Through the Secretion of Various Soluble Factors

FUMITAKA SHIMIZU,[1] YASUTERU SANO,[1] MASA-AKI ABE,[1] TOSHIHIKO MAEDA,[1] SUMIO OHTSUKI,[2] TETSUYA TERASAKI,[2] AND TAKASHI KANDA[1]*

[1]Department of Neurology and Clinical Neuroscience, Yamaguchi University Graduate School of Medicine, Ube, Japan

[2]Department of Molecular Biopharmacy and Genetics, Graduate School of Pharmaceutical Sciences, Tohoku University, Sendai, Japan

The objectives of this study were to establish pure blood–nerve barrier (BNB) and blood–brain barrier (BBB)-derived pericyte cell lines of human origin and to investigate their unique properties as barrier-forming cells. Brain and peripheral nerve pericyte cell lines were established via transfection with retrovirus vectors incorporating human temperature-sensitive SV40 T antigen (tsA58) and telomerase. These cell lines expressed several pericyte markers such as α-smooth muscle actin, NG2, platelet-derived growth factor receptor β, whereas they did not express endothelial cell markers such as vWF and PECAM. In addition, the inulin clearance was significantly lowered in peripheral nerve microvascular endothelial cells (PnMECs) through the up-regulation of claudin-5 by soluble factors released from brain or peripheral nerve pericytes. In particular, bFGF secreted from peripheral nerve pericytes strengthened the barrier function of the BNB by increasing the expression of claudin-5. Peripheral nerve pericytes may regulate the barrier function of the BNB, because the BNB does not contain cells equivalent to astrocytes which regulate the BBB function. Furthermore, these cell lines expressed several neurotrophic factors such as NGF, BDNF, and GDNF. The secretion of these growth factors from peripheral nerve pericytes might facilitate axonal regeneration in peripheral neuropathy. Investigation of the characteristics of peripheral nerve pericytes may provide novel strategies for modifying BNB functions and promoting peripheral nerve regeneration.
J. Cell. Physiol. 226: 255–266, 2010. © 2010 Wiley-Liss, Inc.

Brain and peripheral nerve pericytes, which completely surround capillary endothelial cells, are the critical components of the blood–brain barrier (BBB) and blood–nerve barrier (BNB). Pericytes play important roles in mediating the development, maintenance, and regulation of the BBB and BNB. Pericytes may contribute to the regulation of BBB and BNB–endothelial function by paracrine secretion of growth factors such as Ang I (Davis et al., 1996), TGF-β (Sato and Rifkin, 1989; Hirschi et al., 2003), VEGF (Brown et al., 2001; Reinmuth et al., 2001), and bFGF (Niimi, 2003). In addition, extensive pericyte coverage is found around microvessels in organs that have a barrier system, and the pericyte-to-endothelial ratios are 1:1 in the retina and brain and approximately 1:10 in the lung (Shepro and Morel, 1993). It is not clear why the nervous system requires a larger degree of pericyte coverage than other organs, but one possibility is that brain and peripheral nerve pericytes contribute to the regulation of the BBB and BNB and increase vascular stability.

The loss of pericytes from the microvasculature is one of the earliest hallmarks of several angiopathy-related diseases. Pericyte loss from microvessels is associated with the formation of microaneurysms, microhemorrhage, and local edema in diabetic microangiopathy (Giannini and Dyck, 1995; Lindahl et al., 1997; Hammes, 2005). CADASIL, which is an increasingly recognized autosomal-dominant vascular dementia caused by highly stereotyped mutations in the Notch3 receptor, is a widespread angiopathy characterized by pericyte degeneration. Therefore, clarifying the molecular mechanisms by which pericytes regulate BBB and BNB functions under both physiological and pathological conditions would positively contribute to the development of a novel therapy for many vessel-related diseases such as diabetic microangiopathy and stroke.

Primary cultures of retinal and brain pericytes derived from rat, bovine, and human tissue have been used for in vitro investigation of the physiological roles of pericytes (Capetandes and Gerritsen, 1990; Kondo et al., 2003). Although endoneurial pericytes would be useful sources for investigating the roles of pericytes in pathological conditions such as diabetic neuropathy, no optimal pericyte cell lines originating from the BNB have been developed. This absence is partly due to the difficulty in isolating a sufficient amount of pericytes from a miniscule amount of endoneurial tissue. Recently, brain and peripheral nerve pericyte cell lines were successfully established from rats (Shimizu et al., 2008). However, brain and peripheral nerve pericytes of human tissue origin are definitely necessary in order to study human BBB and BNB function.

The purpose of the present study was to establish pure BBB- and BNB-derived pericyte cell lines from human tissue

origin by transfection with retrovirus vectors incorporating human temperature-sensitive SV40 T antigen (tsA58) and human telomerase (hTERT) and to characterize the established pericyte cell lines. In addition, the differences of cellular properties between brain pericytes originating from the BBB were compared with peripheral nerve pericytes originating from the BNB. In addition, these cell lines up-regulated the barrier function of endothelial cells in the BBB and BNB.

Materials and Methods
Reagents

The culture medium for pericytes was Dulbecco's modified Eagle's medium (DMEM; Sigma, St. Louis, MO) containing 100 U/ml penicillin (Sigma), 100 μg/ml streptomycin (Sigma), 25 ng/ml amphotericin B (Invitrogen, Grand Island, NY), and 10% fetal bovine serum (FBS; Sigma). Polyclonal anti-NG2, anti-Ang-1, anti-BDNF, and anti-GDNF antibodies were obtained from Santa Cruz (Santa Cruz, CA). Monoclonal anti-SV40 antibody was purchased from Calbiochem (Darmstadt, Germany). Monoclonal anti-SMA antibody and polyclonal anti-vWF antibody were obtained from Dako (A/S,Glostrup, Denmark). Polyclonal anti-claudin-5 and anti-occludin antibodies were purchased from Zymed (San Francisco, California). Polyclonal anti-bFGF, anti-TGF-β, and anti-VEGF antibodies were purchased from R&D Systems (Minneapolis, Minnesota). Recombinant human TGF-β, Ang-1, VEGF, bFGF, and TNF-α were purchased from Peprotech EC (London, UK). Human umbilical vein ECs (HUVEC) and HL-60 cells were obtained from Japan Health Sciences Foundation (Osaka, Japan), and human astrocytes were purchased from Lonza (Walkersville, Maryland). TY10 cells were conditionally immortalized a brain microcapillary endothelial cell line (BMECs) (Sano et al., 2010), and used as in vitro BBB model. Primary human fibroblasts were obtained from DS Pharma Biomedical (Osaka, Japan).

Isolation of peripheral nerve and brain pericytes and establishment of cell lines

The study protocol for human tissue was approved by the ethics committee of the Medical Faculty, University of Yamaguchi Graduate School and was conducted in accordance with the Declaration of Helsinki, as amended in Somerset West in 1996. Written informed consent was obtained from the family of the participants before entering the study.

Human sciatic nerve and brain tissues samples were obtained from a patient who suddenly died from a heart attack. The isolation procedure follows that of the previous method with modification (Kanda et al., 1997). Briefly, the sciatic nerve was removed and the endoneurium was carefully separated from the epineurium and perineurium using fine forceps, dissected into small pieces, and digested with 0.25% type I collagenase (Sigma). After

centrifugation, the mixture was centrifuged, and the pellet was suspended in 15% dextran solution. The pellet was resuspended and cell suspension placed onto a type I collagen-coated dish (Becton Dickinson, Tokyo, Japan). The brain capillary-rich fractions were isolated using a previously reported method (Kanda et al., 1994). Briefly, the cerebral cortex of the human brain was homogenized, and the homogenate was further dissociated with 0.005% dispase (Sigma). After the mixture was centrifuged, the pellet was suspended in 15% dextran solution. Next, the pellet was resuspended and the cell suspension was filtered through a 190-μm nylon mesh, and the filtered cell clusters were plated onto a type I collagen-coated dish. The colonies of pericyte and peripheral nerve microvascular endothelial cells (PnMECs) were isolated using a cloning cap. Pure peripheral nerve and brain pericytes, and PnMECs were isolated after two or three passages. Thereafter, peripheral nerve and brain pericytes were immortalized via sequential transduction with retrovirus-incorporated tsA58 and hTERT genes. Pericytes were initially incubated overnight with a high concentration of retrovirus vector carrying tsA58 in 10% DMEM. The cells were subsequently washed, and the temperature was adjusted from 37 to 33°C to activate the large T-antigen. This process was followed by another overnight incubation with a high concentration of retrovirus vector carrying hTERT.

Reverse transcription-polymerase chain reaction (RT-PCR) analysis

Total RNA was extracted using an RNeasy® Plus Mini Kit (Qiagen, Hilden, Germany) following the manufacturer's protocol. Single-stranded cDNA was created from 40 ng total RNA by StrataScript First Strand Synthesis System (Stratagene®, Cedar Greek, TX). The sequence specificity of each human primer pair and its reference are shown in Table 1. RT-PCR amplification was performed using TAKARA PCR Thermal Cycler Dice (Takara, Otsu, Japan). The RT-PCR amplification products were separated by electrophoresis in 2% agarose gels containing 0.5 mg/ml ethidium bromide and visualized with an imager.

Quantitative real-time PCR analysis

A quantitative real-time PCR analysis was performed using a Stratagene's Mx3005P (Stratagene®) with FullVelocity® SYBR® Green QPCR master mix (Stratagene®) according to the manufacturer's protocol. The sequences of primers are shown in Table 1. Glyceraldehyde-3-phosphate dehydrogenase (GAPDH) was used as an internal standard. The samples were subjected to PCR analysis using the following cycling parameters: 95°C for 10 min, 95°C for 15 sec, and 60°C for 1 min for 40 cycles. Negative controls (cDNA-free solutions) were included in each reaction. The standard reaction curve was analyzed by MxPro^{TM} (Stratagene®) software and the relative quantity according to standard reaction curve (R_v) was calculated according to the formula $R_v = R_{Gene}/R_{GAPDH}$ by computer.

TABLE 1. Human primer pairs utilized in RT-PCR analysis

Target	Sense	Antisense	Refs.
PDGF-β	5′-AATGTCTCCAGCACCTTCGT-3′	5′-AGCGGATGTGGTAAGGCATA-3′	Basciani et al. (2002)
Osteopontin	5′-ACCCTCTCTGACACCCTGTG-3′	5′-GGCTGGCTTCTCACATTCTC-3′	Said et al. (2007)
Ang-I	5′-GGAAGTCTAGATTTCCAAAGAGGC-3′	5′-CTTTATCCCATTCAGTTTTCCATG-3′	Huang et al. (2000)
TGF-β1	5′-ACCAACTATTGCTTCAGCTC-3′	5′-TTATGCTGGTTGTACAGG-3′	Soufla et al. (2005)
VEGF	5′-GCAGAAGGAGGAGGGCAGAATC-3′	5′-ACACTCCAGGCCCTCGTCATT-3′	Soufla et al. (2005)
BFGF	5′-GAAGAGCGACCCTCACATCAAG-3′	5′-CTGCCCAGTTCGTTTCAGTG-3′	Soufla et al. (2005)
NGF	5′-TCATCATCCCATCCCATCTT-3′	5′-CTTGACAAAGGTGTGAGTCG-3′	Bronzetti et al. (2006)
BDNF	5′-AGCCTCCTCTGCTCTTTCTGCTGGA-3′	5′-CTTTTGTCTATGCCCCTGCAGCCTT-3′	Bronzetti et al. (2006)
GDNF	5′-CGCCGCCGGACGGGACTTTAAGATGAAGTTA-3′	5′-CAAGAGCCGCTGCAGTACCTAAAAATCA-3′	Bäckman et al. (2006)
VWF	5′-CACCATTCAGCTAAGAGGAGG-3′	5′-GCCCTGGCAGTAGTGGATA-3′	Fuchs et al. (2006)
Claudin-5	5′-CTGTTTCCATAGGCAGAGCG-3′	5′-AAGCAGATTCTTAGCCTTCC-3′	Varley et al. (2006)
Occludin	5′-TGGGAGTGAACCCAACTGCT-3′	5′-CTTCAGGAACCGGCGTGGAT-3′	Ghassemifar et al. (2003)
G3PDH	5′-TGAAGGTCGGAGTCAACGGATTTGGT-3′	5′-CATGTGGGCCATGAGGTCCACCAC-3′	Ye (2003)
GAPDH (real-time)	5′-GTCAA CGGAT TTGGT CTGTA TT-3′	5′-AGTCT TCTGG GTGGC AGTGAT-3′	Zhang et al. (2006)

Western blot analysis

The proteins samples (10–20 μg) were separated by SDS–PAGE (Biorad, Tokyo, Japan), and transferred to nitrocellulose membrane (Amersham, Chalfont, UK). The membranes were treated with blocking buffer (5% skimmed milk in 25 mM Tris–HCl, pH 7.6, 125 nM NaCl, 0.5% Tween-20) for 1 h at room temperature and incubated with relevant antibodies (dilution 1:100) for 2 h at room temperature as the primary antibodies. The membrane were exposed to peroxidase-conjugated secondary antibody (1:2,000) followed by chemiluminescence reagent (Amersham), exposure to X-Omat S films (Amersham), and quantification of bands intensity using the Fuji image analysis software package.

Immunocytochemistry

The cultured cells were fixed with 4% paraformaldehyde (Wako, Osaka, Japan) and were permeabilized with 100% methanol. The cells were subsequently incubated overnight with relevant antibodies (dilution 1:50–100), and then incubated with FITC-labeled secondary antibody at dilution of 1:200 staining. The fluorescence was observed by a fluorescent microscope (Olympus, Tokyo, Japan). The nuclei were stained with DAPI, and the fluorescence was detected with a fluorescence microscope (Olympus). Image stacks were analyzed with the localization module of the Olympus software program (Olympus).

Uptake of Dil-Ac-LDL

The cells were incubated with cultured media containing 10 μg/ml acetylated low-density lipoprotein labeled 1,1′-dioctadecyl-3,3,3′,3′-tetramethyliodo-carbocyanine perchlorate (Dil-Ac-LDL; Biogenesis, Poole, England) at 37°C for 12 h. After incubation, the cells were photographed using a fluorescent microscope (Olympus).

Treatment of PnMECs with a conditioned medium of pericyte, angiopoietin-1, VEGF, or bFGF, and exposure of pericytes with TNF-α

The brain and peripheral nerve pericytes, astrocyte, and fibroblasts were cultured in DMEM with 20% FBS. After 24 h, the conditioned medium of brain pericytes (BPCT-CM), peripheral nerve pericytes (PPCT-CM) astrocytes (AST-CM), and fibroblasts (fibro-CM) was collected and stored at −20°C until analysis. The control medium was prepared by the same procedure using DMEM with 20% FBS (non-conditional medium (NCM)). PnMECs were treated with NCM, BPCT-CM, or PPCT-CM, or treated with angiopietin-1 (0, 0.1, 1, and 10 ng/ml), VEGF (0, 0.1, 1, and 10 ng/ml), or bFGF (0, 0.1, 1, and 10 ng/ml). Peripheral nerve pericytes were treated with DMEM with 10% FBS (NCM) and TNF-α (100 ng/ml). The total RNA was extracted 24 h later, and total protein was obtained after 3 days.

bFGF inhibitory study

PnMECs were cultured with PPCT-CM containing 1.0 μg/ml antibody against bFGF or normal rabbit IgG. The total RNA was extracted 24 h later, and total protein was obtained 3 days later.

Transendothelial electrical resistance (TEER) study

Transwell inserts (pore size 0.4 μm, effective growth area 0.3 cm², BD Bioscience, Franklin Lakes, NJ) were coated by rat-tail collagen type-I (BD Bioscience) according to the manufacturer's instructions. After PnMECs were seeded (1 × 10⁶ cells/insert) in the upper compartment and cultured for 24 h, the upper compartment was incubated with each medium (NCM, EBM, BPCT-CM, and PPCT-CM) for 3 days. To construct in co-culture system, brain and peripheral nerve pericytes, astrocytes, or fibroblasts were seeded on the bottom side of the inserts. The cells were allowed to adhere firmly for overnight, and then endothelial cells were seeded on the upper side of the inserts placed in the well

of the 24-well culture plates containing no cells, pericytes, or astrocytes. TEER values of cell layers were measured with a Millicell electrical resistance apparatus (Endohm-6 and EVOM; World Precision Instruments, Sarasota, FL). Statistical significance was evaluated using Student's t-test.

Transendothelial transport study

The paracellular passage of ^{14}C-labeled inulin (0.2 μCi/ml) across the cell layers was determined using previously described protocols. After 0.2 μCi of [carboxyl-^{14}C]-inulin in 0.5 ml of DMEM was added to the upper compartment, the appearance of [carboxyl-^{14}C]-inulin in the lower chamber was measured after 20 min by scintillation counting of 20 μl samples from the upper and lower chambers. The clearance (in μl) of inulin (C_{inu}) was calculated as $C_{inu} = V_L{}^* CPM_L / CPM_U$, where V_L is the volume of the lower compartment in μl, CPM_L is the radioactivity of [carboxyl-^{14}C]-inulin in the lower chamber in $CPM/μl$, and CPM_U is the radioactivity of [carboxyl-^{14}C]-inulin in the upper compartment in $CPM/μl$. The upper compartment was incubated with each medium (NCM, EBM, BPCT-CM, and PPCT-CM) for 3 days.

Data analysis

All data are presented as the mean ± SEM. The unpaired, two-tailed Student's t-test was used to determine the significance of differences between two group means. A P-value of <0.01 was considered to be statistically significant.

RESULTS
Characterization of human peripheral nerve and brain pericyte cell lines

Human peripheral nerve and brain pericyte cell lines were established (Fig. 1A–C). These two cell lines appeared to have a ruffled-border morphology with highly irregular edges, as shown in Figure 1A,B. The expression of the endothelial cell markers, vWF and PECAM, was not detected by RT-PCR in either cell line (Fig. 2A) and vWF expression was not detected by immunocytochemistry (Fig. 1D,E). These cell lines also did not take up Dil-Ac-LDL (Fig. 1G,H), thus indicating that they did not have the Ac-LDL receptor, which is an essential endothelial cell marker. We therefore confirmed that these cell lines were not contaminated by endothelial cells. We also isolated PnMECs of human BNB origin (Fig. 1C). Approximately 100% of the cells were immunoreactive for wWF (Fig. 1F) and they displayed the uptake of Dil-Ac-LDL (Fig. 1I).

The mRNA of several pericyte markers, such as PDGF-Rβ, desmin, and osteopontin, was detected by RT-PCR in the pericyte cell lines as well as in human brain tissue used as a positive control (Fig. 2A). The expression of αSMA and NG2 in these cell lines was verified by Western blot analysis (Fig. 2B,C) and immunocytochemistry (Fig. 2D,E) (Nehls and Drenckhahn, 1991; Ozerdem et al., 2001). They displayed stable growth and differentiated characteristics after at least five passages.

The peripheral nerve and brain pericytes cell lines expressed a large T-antigen with a molecular weight of 94 kDa under a permissive temperature of 33°C, which was the same molecular weight as that expressed by TR-BBB13 which expresses T-antigen at 33°C as a positive control (Hosoya et al., 2000) (Fig. 2F). Although hTERT protein was not detected by Western blot analysis (data not shown), these cell lines displayed a high expression level of nuclear and perinuclear hTERT protein by confocal microscopy (Fig. 2G,H). Therefore, pure BBB- and BNB-derived pericyte cell lines were successfully established from human tissue and identified the characteristics of the established pericyte cell lines.
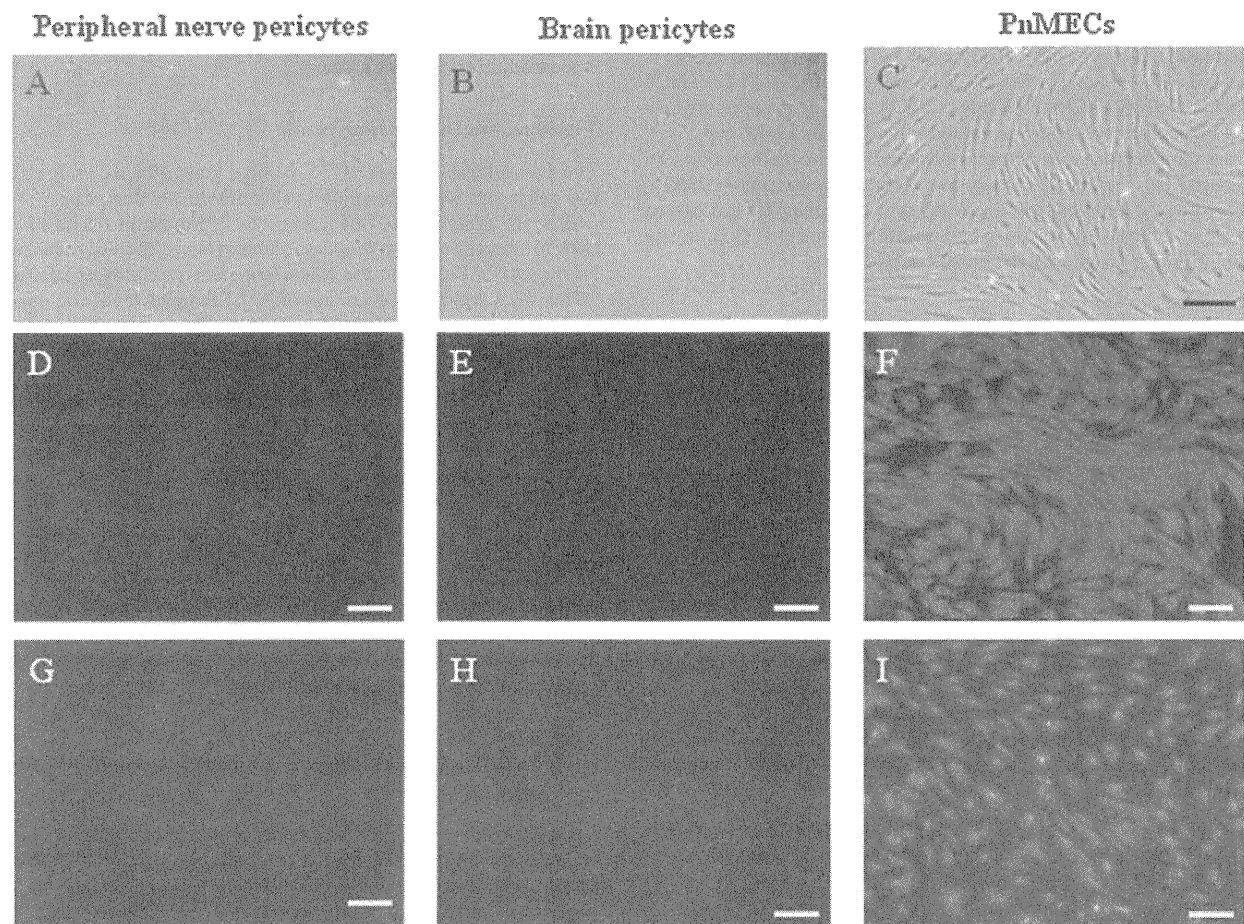
Fig. 1. A phase microscopic image of human peripheral nerve pericytes (A,D,G), brain pericytes (B,E,H), and PnMECs (C,F,I). Pericytes appeared to have ruffled-border morphology (A,B). Anti-vWF antibody did not stain peripheral nerve (D) or brain pericytes (E). PnMECs were used as a positive control (F). No uptake of Dil-Ac-LDL was observed in peripheral nerve (G) or brain pericytes (H). PnMECs were used as a positive control (I). [Color figure can be viewed in the online issue, which is available at wileyonlinelibrary.com.]

Paracrine growth factor and nerve growth factor secreted from the brain and peripheral nerve pericytes

The expression levels of the mRNA of pericyte paracrine growth factors such as Ang-1, TGF-β1, VEGF, and bFGF in the isolated pericytes are shown in Figure 3A.

In addition, the expression of Ang-1, TGF-β1, VEGF, and bFGF proteins in these pericyte cell lines was determined by a Western blot analysis (Fig. 3B). The Ang-1, TGF-β, VEGF, and bFGF bands, corresponding to 60-, 25-, 38-, and 16-kDa single bands, respectively, were detected in the brain and peripheral nerve pericytes, and astrocytes. The Ang-1, TGF-β, and bFGF bands, corresponding to this band, were not detected in PnMECs. Interestingly, the levels of Ang-1 (Fig. 3C), TGF-β (Fig. 3D), and bFGF (Fig. 3F) proteins in peripheral nerve pericytes were significantly higher than those in brain pericytes (P < 0.01; Fig. 3C,D,F). Their levels were almost equivalent to those in astrocytes. In contrast, the expression of VEGF protein did not show a significant difference between these cell lines (Fig. 3E). This study also investigated whether these pericyte cell lines expressed neurotrophic factors to promote nerve regeneration. The mRNA expression levels of nerve growth factors such as GDNF, NGF, and BDNF were determined in brain and peripheral nerve pericytes and shown in Figure 4A. These

GDNF and NGF were not detected in PnMECs (Fig. 4A). Interestingly, the GDNF (Fig. 4B) and NGF (Fig. 4C) mRNA expression levels in peripheral nerve pericytes were significantly higher than those in brain pericytes (P < 0.01). Their levels were almost equivalent to those in astrocytes. Furthermore, the BDNF (Fig. 4D) mRNA expression level in the brain and peripheral nerve pericytes was also significantly higher than that in PnMECs (P < 0.01) and it was also equivalent to that in astrocytes. In addition, the expression of GDNF and BDNF proteins in the isolated pericytes was determined by a Western blot analysis (Fig. 4E). The GDNF and BDNF bands, corresponding to 15- and 14-kDa single bands, respectively, were detected in the brain and peripheral nerve pericytes, and astrocytes (Fig. 4E). The GDNF and BDNF bands were not detected in PnMECs. Interestingly, the levels of GDNF (Fig. 4F) and BDNF (Fig. 4G) protein in peripheral nerve pericytes were significantly higher than those in brain pericytes (P < 0.01) and astrocytes (P < 0.01). The change in GDNF, BDNF, and NGF mRNA in peripheral nerve pericytes after treatment with TNF-α (100 ng/ml) was measured using relative quantification with real-time RT-PCR (Fig. 4H–J). The GDNF (Fig. 4H), BDNF (Fig. 4I), and NGF (Fig. 4J) mRNA expression levels in the peripheral nerve pericytes significantly increased after treatment with TNF-α (P < 0.01).
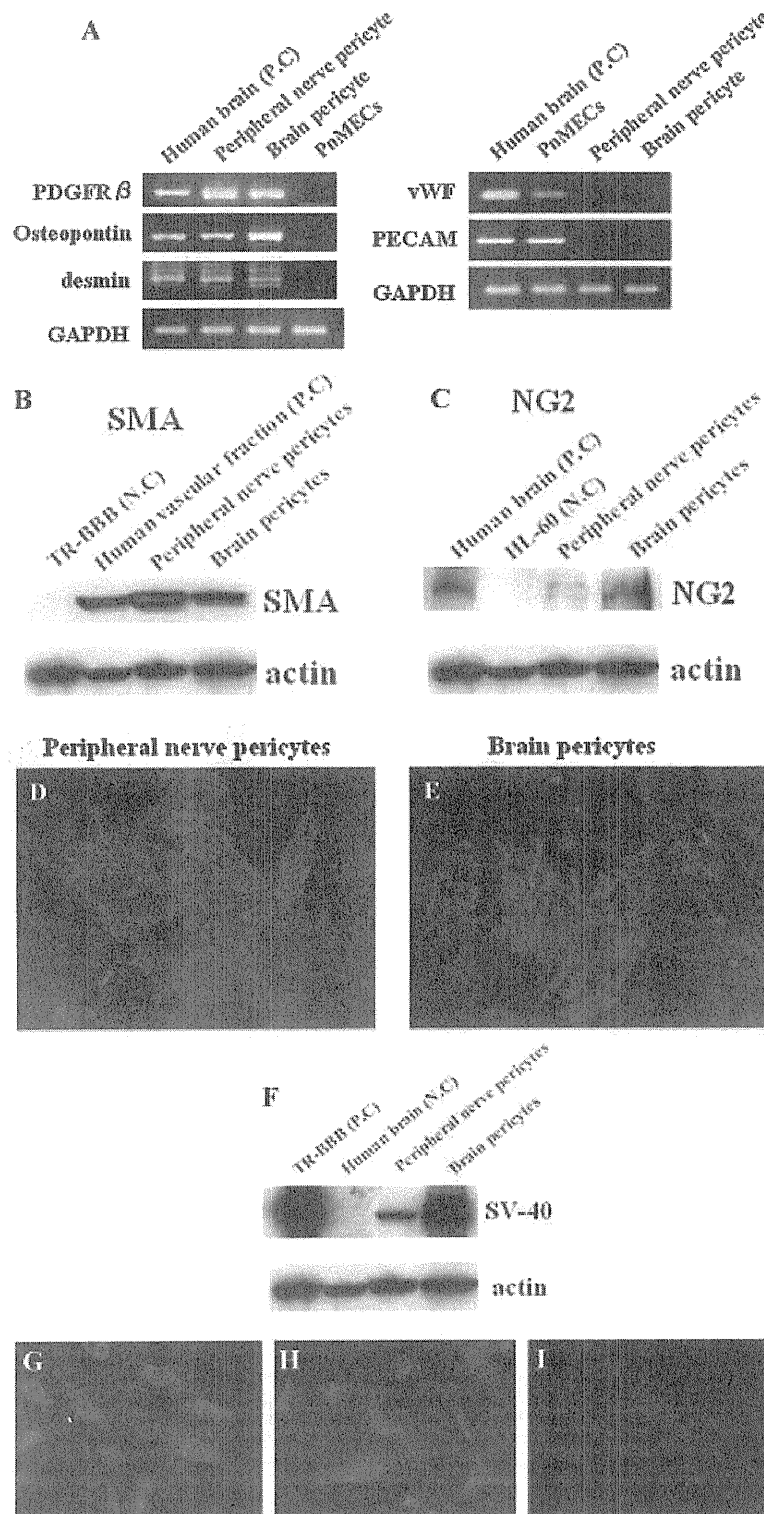
Fig. 2. A: The expression of pericyte markers, including PDGF-Rβ, osteopontin, and desmin, and of vWF and PECAM as endothelial cell markers by RT-PCR analysis. Human brain tissue was used as a positive control, and PnMECs were used as a negative control. Each mRNA expression level was normalized with respect to the GAPDH mRNA expression. A Western blot analysis of αSMA (B) and NG2 (C) proteins in pericyte cell lines. Human vascular fraction and human brain tissue were used as positive controls, and TR-BBB and HL-60 cells were used as negative controls. Immunocytochemistry using anti-αSMA antibody against peripheral nerve (D) and brain pericytes (E,F) The expression of a large SV40 T-antigen in peripheral nerve and brain pericytes cultured at 33°C. TR-BBB cultured at 33°C was used as a positive control and human brain tissue was used as a negative control. G,H,I: The presence of nuclear and perinuclear hTERT was confirmed by immunocytochemistry using anti-hTERT antibody in peripheral nerve (G) and brain (H) pericyte cell lines. HUVEC was used as a negative control (I). [Color figure can be viewed in the online issue, which is available at wileyonlinelibrary.com.]
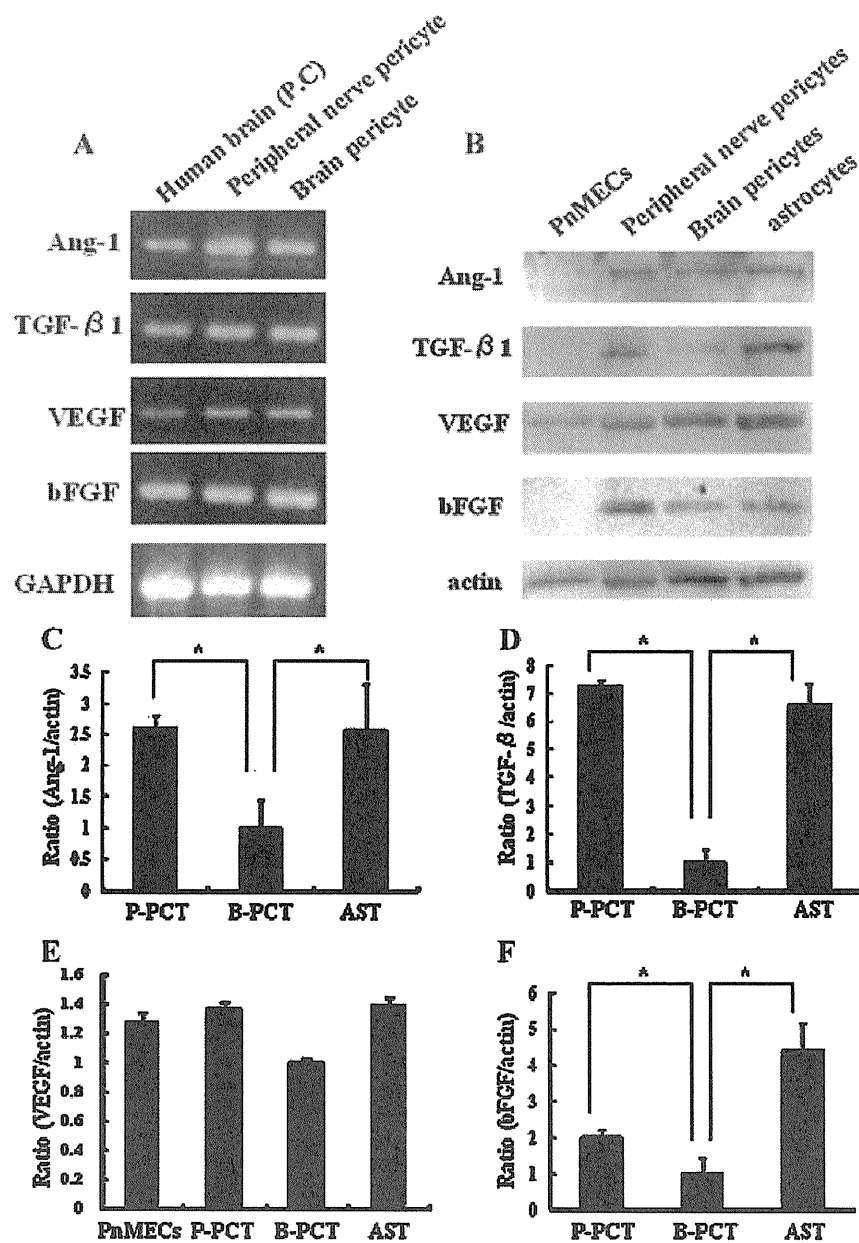
Fig. 3.   A: The expression of the paracrine growth factors Ang-1, TGF-β, VEGF, and bFGF by RT-PCR analysis. Human brain tissue was used as a positive control. Each mRNA level was normalized with respect to the expression of GAPDH mRNA. Human brain served as a positive control (P.C). B: A Western blot analysis of Ang-1, VEGF, TGF-β, and bFGF in peripheral nerve and brain pericyte, PnMECs, and astrocyte. The Ang-1, TGF-β, VEGF, and bFGF bands, corresponding to 60-, 25-, 38-, and 16-kDa single bands, respectively, were detected in the brain and peripheral nerve pericytes, and astrocytes. The Ang-1, TGF-β, and bFGF proteins corresponding to this band were not detected in PnMECs. C–F: The bar graph reflects the combined densitometry data from three independent experiments (mean ± SEM, n = 3, *P < 0.01). B,C: The Ang-1, TGF-β, and bFGF protein levels in peripheral nerve pericytes were significantly higher than those in brain pericytes (mean ± SEM, n = 3, *P < 0.01).

The change of TEER and transendothelial permeability of PnMECs by pericyte-conditioned medium

The TEER and permeability for paracellular diffusion of [carboxyl-C14]-inulin across the layer of PnMECs or TY08 in response to treatment with NCM, BPCT-CM, and PPCT-CM (Fig. 5A–E) was measured to determine whether soluble factors secreted by pericytes strengthen the barrier function of endothelial cells in the BBB or BNB. The TEER value of TY08

was not changed after treatment with fibroblast (FB)-CM, but significantly increased after incubation with AST-CM or BPCT-CM (P < 0.01; Fig. 5A). There was no significant difference in the TEER value after treatment of TY08 with AST-CM and BPCT-CM. When cultured with BPCT-CM or PPCT-CM, the TEER value of PnMECs was also significantly elevated (P < 0.01) in comparison to those treated with NCM, although it was not changed after exposure of FB-CM (Fig. 5B). The transfilter co-culture of TY08 with brain pericytes or astrocytes could
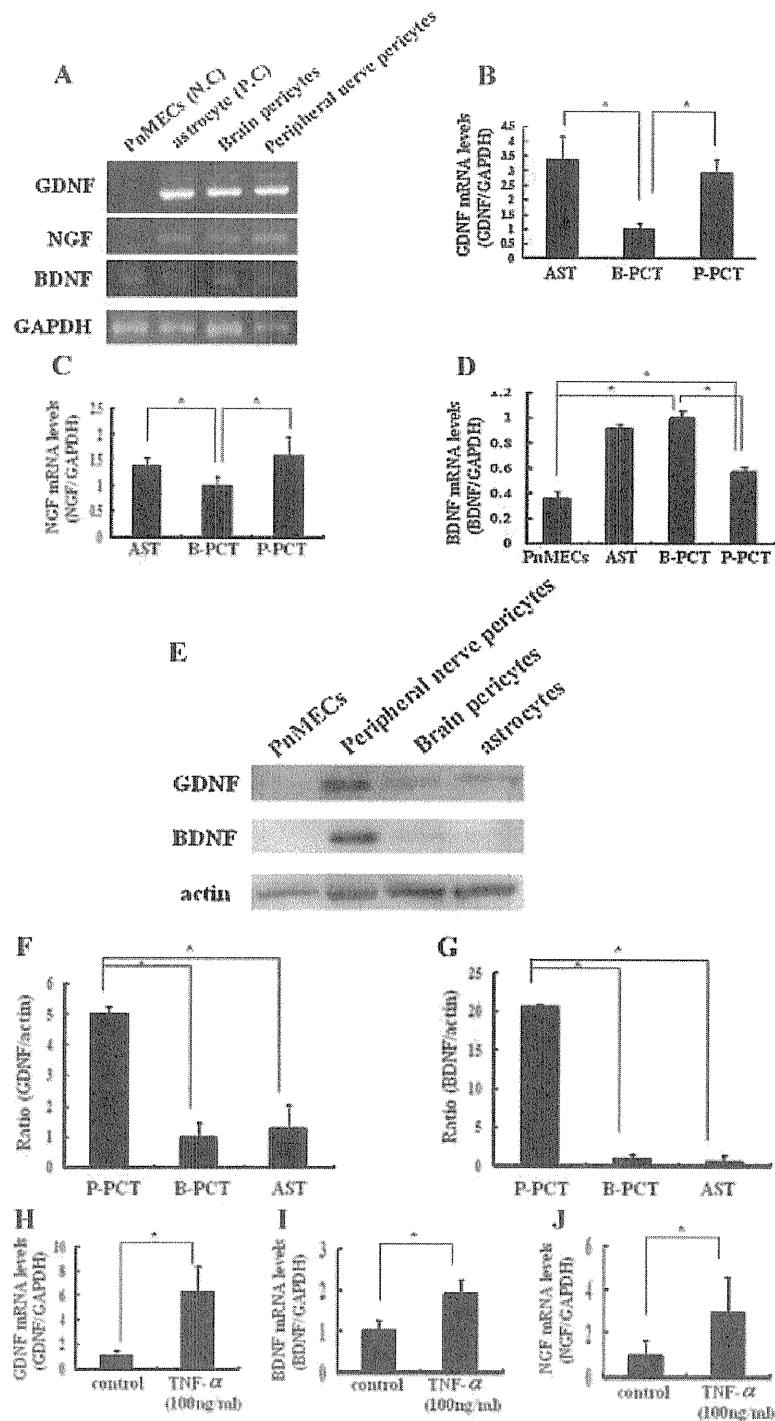
Fig. 4. A: The expression of paracrine growth factors, including GDNF, NGF, and BDNF, by RT-PCR analysis. Human brain tissue was used as a positive control. The mRNA expression levels were normalized with respect to the expression of GAPDH mRNA. The expression of GDNF and NGF mRNA was not detected in PnMECs. Astrocytes served as a positive control (P.C) and PnMECs as a negative control (N.C). B–D: GDNF, NGF, and BDNF mRNA levels were quantified in brain pericytes, peripheral nerve pericytes, PnMECs, and astrocytes by real-time RT-PCR expressed as the ratio of target gene/GAPDH. B,C: The GDNF and NGF mRNA expression levels in peripheral nerve pericytes were equivalent to those in astrocytes and significantly higher than those in brain pericytes (mean ± SEM, n = 3, *P < 0.01). D: The BDNF mRNA expression levels in brain and peripheral nerve pericytes were also equivalent to that in astrocytes and significantly higher than those in PnMECs (mean ± SEM, n = 3, *P < 0.01).
E: A Western blot analysis of GDNF and BDNF protein in peripheral nerve and brain pericytes, PnMECs, and astrocytes. The GDNF and BDNF bands, corresponding to 15- and 14-kDa single bands, respectively, were detected in the brain and peripheral nerve pericytes, and astrocytes. F,G: The bar graph reflects the combined densitometry data from three independent experiments (mean ± SEM, n = 3, *P < 0.01). The GDNF and BDNF protein levels in peripheral nerve pericytes were significantly higher than those in brain pericytes and astrocyte (mean ± SEM, n = 3, *P < 0.01). The GDNF and BDNF proteins corresponding to this band were not detected in PnMECs. H–J: The GDNF, BDNF, and NGF mRNA expression levels in peripheral nerve pericytes were significantly increased after treatment with TNF-α (P < 0.01).
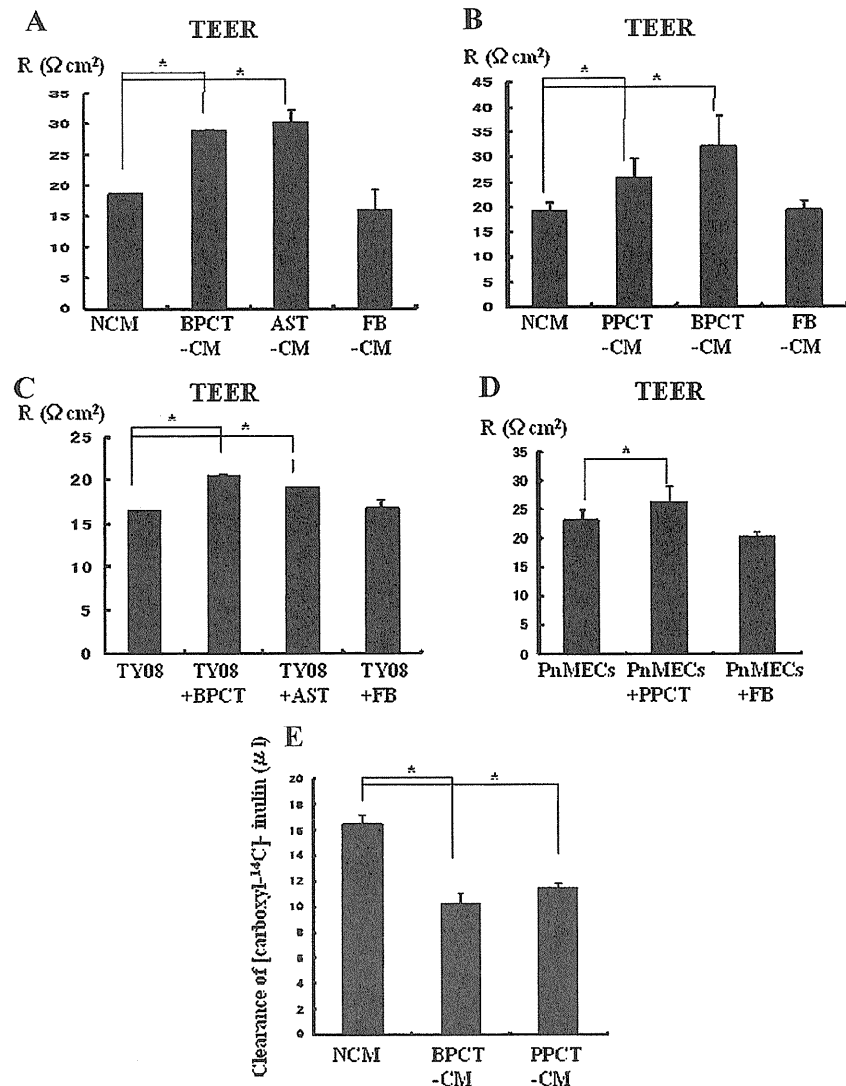
Fig. 5.   A: The effect of brain pericytes and astrocytes-conditioned media on the TEER values across TY08 monolayer (mean ± SD, n = 6 in each condition). The TEER value of TY08 was not changed after treatment with fibroblast (FB)-CM, but significantly increased after incubation with AST-CM and BPCT-CM (P < 0.01). B: The effect of brain and peripheral nerve pericyte-conditioned media on the TEER values across PnMEC monolayer (mean ± SD, n = 6 in each condition). The TEER values of PnMECs were significantly increased when cultured with brain or peripheral nerve pericyte-conditioned media. C: The effect of co-culture on induction of TEER in TY08 with brain pericytes or astrocytes. High TEER was observed in the co-culture of TY08 with brain pericytes or astrocytes in comparison to endothelial cell monolayer (P < 0.01). The TEER value of TY08 was not changed by co-culture with fibroblasts. D: The effect of co-culture on induction of TEER in PnMECs with peripheral nerve pericytes. The TEER value of PnMECs was not changed after co-culture with fibroblast, but significantly increased after co-culture with peripheral nerve pericytes (P < 0.01). E: The [carboxyl-^{14}C]-inulin clearance of the PnMEC monolayer treated with brain or peripheral nerve pericyte-conditioned media at 30 min (mean ± 6 in each experiment). PnMECs demonstrated a significantly lower inulin clearance when cultured with brain or peripheral nerve pericyte-conditioned media (*P < 0.01). NCM, Non-conditioned medium was prepared by the same procedure using DMEM with 10% FBS; BPCT-CM, conditioned medium of brain pericytes; PPCT-CM, conditioned medium of peripheral nerve pericytes; AST-CM, conditioned medium of astrocytes; FB-CM, conditioned medium of fibroblasts. TY08, Monoculture of TY08; TY08 + BPCT, co-culture of TY08 with brain pericytes; TY08 + AST, co-culture of TY08 with astrocytes; TY08 + FB, co-culture of TY08 with fibroblasts; PnMECs, monoculture of PnMECs; PnMECs + PPCT, co-culture of PnMECs with peripheral nerve pericytes; PnMECs + FB, co-culture of PnMECs with fibroblasts.

significantly increase the tightness of endothelial monolayers (P < 0.01; Fig. 5C). High TEER was observed in the co-culture of PnMECs with peripheral nerve pericytes in comparison to endothelial cell monolayer (P < 0.01; Fig. 5D). The TEER values of TY08 and PnMECs were unchanged by co-culture with fibroblasts in comparison to the single culture (Fig. 5C,D). Furthermore, PnMECs treated with BPCT-CM or PPCT-CM demonstrated significantly lower inulin clearance than those treated with NCM (P < 0.01; Fig. 5E).

Induction of claudin-5 and occludin in PnMECs following treatment with the pericyte-conditioned medium

Changes in the expression of claudin-5 and occludin mRNA in PnMECs following treatment with NCM, BPCT-CM, and PPCT-CM were examined to determine whether soluble factors secreted from pericytes up-regulate the expression of tight junctional molecules (Fig. 6A,B). The claudin-5 and occludin
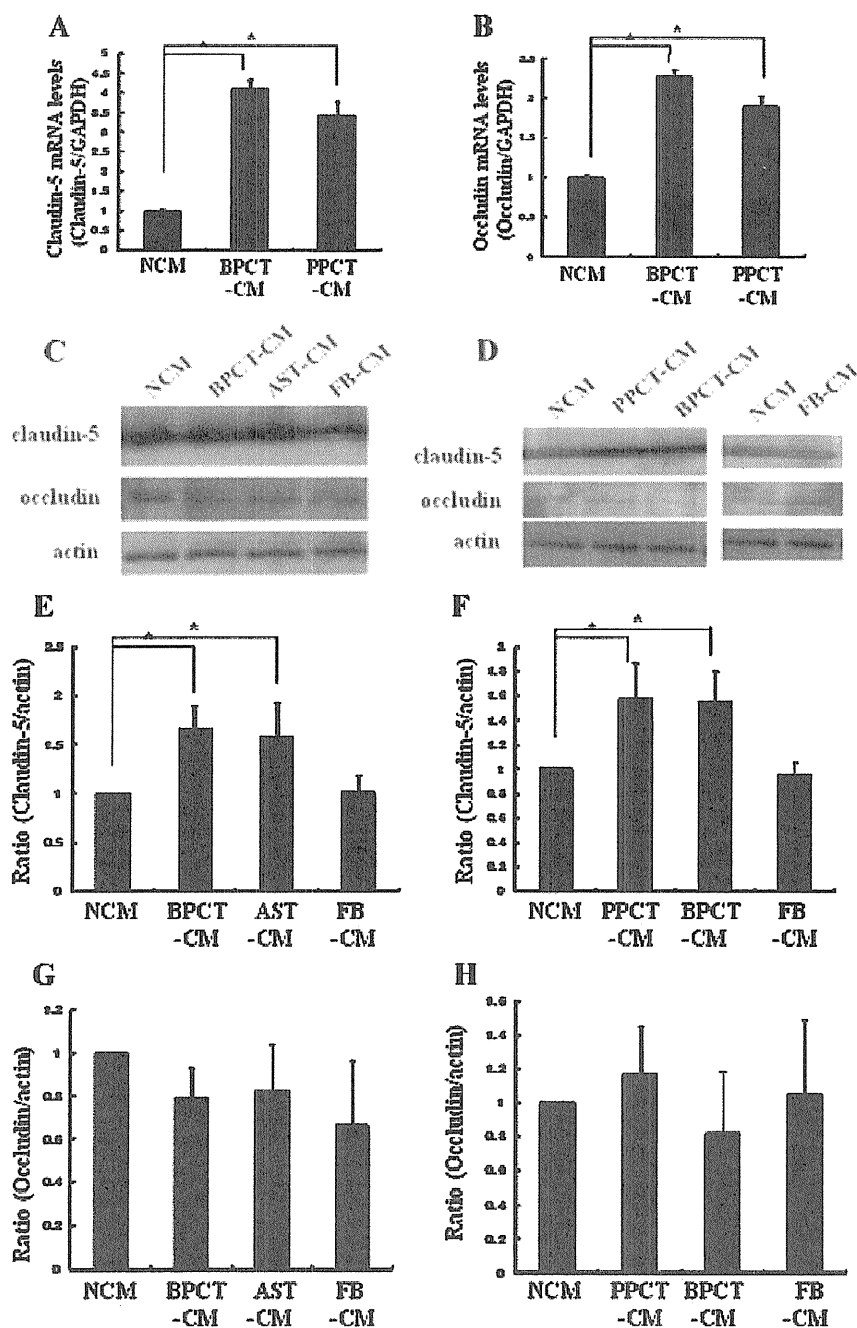
Fig. 6. Effect of brain and peripheral nerve pericyte-conditioned media on the mRNA expression of claudin-5 (A) and occludin (B) by real-time RT-PCR expressed as the ratio of target gene/GAPDH. The expression of claudin-5 and occludin in PnMECs was significantly increased when cultured with brain or peripheral nerve pericyte-conditioned medium. The change of claudin-5 (C) and occludin (D) expression in TY08 or PnMECs treated with BPCT-CM, PPCT-CM, AST-CM, or FB-CM. E–H: The bar graph reflects the combined densitometry data from three independent experiments (mean ± SEM, n = 3, $^*P < 0.01$). E: Claudin-5 of TY08 was not changed following treatment with FB-CM, but those of TY08 was induced after incubation with AST-CM or BPCT-CM ($P < 0.01$). F: The expression of claudin-5 of PnMECs was significantly increased when cultured with BPCT-CM or PPCT-CM, although it was unchanged after application with FB-CM (mean ± SEM, n = 3, $^*P < 0.01$). G,H: The expression of occludin in TY08 or PnMECs was unchanged following treatment with BPCT-CM, PPCT-CM, or AST-CM. NCM, Non-conditioned medium was prepared by the same procedure using DMEM with 10% FBS; BPCT-CM, conditioned medium of brain pericytes; PPCT-CM, conditioned medium of peripheral nerve pericytes; AST-CM, conditioned medium of astrocytes; FB-CM, conditioned medium of fibroblasts.

mRNA expression levels in PnMECs were increased significantly after treatment with BPCT-CM or PPCT-CM ($P < 0.01$; Fig. 6A,B). In addition, the change in claudin-5 and occludin proteins in TY08 and PnMECs treated with NCM, BPCT-CM, PPCT-CM, AST-CM, and FB-CM was determined by a Western blot analysis (Fig. 6C,D). Claudin-5 of TY08 was not changed following treatment with FB-CM but was induced after incubation with AST-CM or BPCT-CM ($P < 0.01$)

(Fig. 6E). There was no significant difference in the amount of claudin-5 after treatment of TY08 with AST-CM and BPCT-CM. When cultured with BPCT-CM or PPCT-CM, the expression of claudin-5 of PnMECs was significantly increased (Fig. 6F). In contrast, occludin was not affected following treatment with BPCT-CM, PPCT-CM, or AST-CM (Fig. 6G,H).

Regulation of claudin-5 by Ang-I, VEGF, TGF-β, and bFGF and the effect of anti-bFGF antibody on the induction of claudin-5 mRNA in PCT-CM-treated PnMECs

The effects of 24 h treatment of Ang-I, VEGF, TGF-β, and bFGF on the expression of claudin-5 mRNA in PnMECs were investigated to determine which soluble factors secreted from pericytes strengthened barrier function in the BBB and BNB. The claudin-5 mRNA level was significantly reduced following treatment with Ang-I, VEGF, and TGF-β in a dose-dependent manner (Fig. 7A–C). Conversely, claudin-5 mRNA was increased following treatment with bFGF (Fig. 7D). Furthermore, claudin-5 protein in PnMECs following treatment with Ang-I (I ng/ml), VEGF (I ng/ml), TGF-β (I ng/ml), and bFGF (I ng/ml) was quantified using a Western blot analysis (Fig. 7E). Claudin-5 protein was significantly increased after treatment with bFGF ($P < 0.01$; Fig. 7E,F). In contrast, claudin-5 protein was significantly reduced following treatment with VEGF, Ang-I, or TGF-β ($P < 0.01$; Fig. 7E,F). The TEER value of PnMECs by treatment with bFGF was significantly higher ($P < 0.01$) in comparison to those treated with NCM (Fig. 7G). Conversely, the TEER value of PnMECs was significantly reduced following treatment with VEGF, Ang-I, or TGF-β (Fig. 7G). To clarify the contribution of bFGF to the induction of claudin-5 in PnMECs by PPCT-CM, bFGF activities were neutralized using anti-bFGF antibody. The claudin-5 mRNA expression was inhibited by 42% after incubation with PPCT-CM pretreated by anti-bFGF antibody (Fig. 7H). In addition, claudin-5 protein in PnMECs following treatment with anti-bFGF neutralizing antibody was quantified using a Western blot analysis (Fig. 7I,J). Claudin-5 protein expression was inhibited after pretreatment with anti-bFGF neutralizing antibody (Fig. 7I,J). The TEER value of PnMECs was also significantly reduced following treatment with PPCT-CM pretreated with anti-bFGF neutralizing antibody (Fig. 7K).
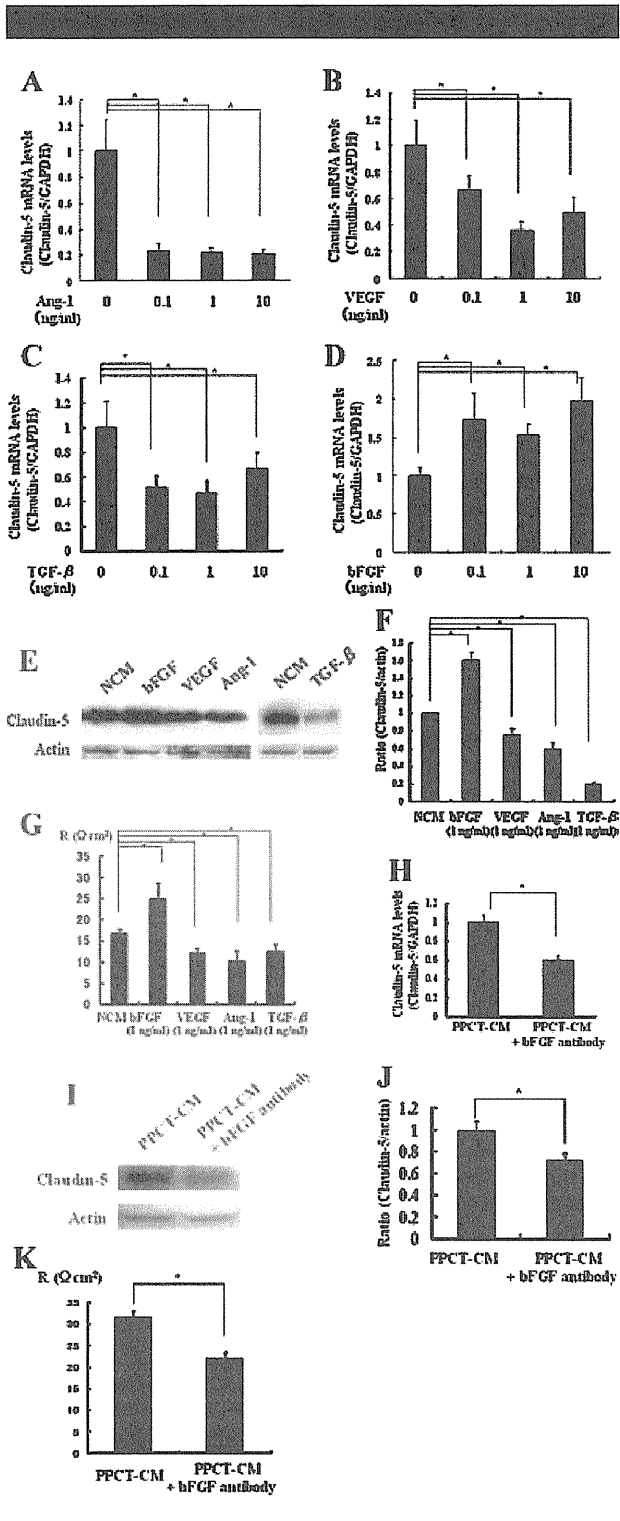

Fig. 7. The claudin-5 mRNA level after a 24-h application of VEGF, Ang-I, TGF-β, and bFGF in PnMECs. A–D: The claudin-5 mRNA levels in PnMECs were quantified by real-time RT-PCR and expressed as the ratio of target gene/GAPDH. Data are presented as the mean (±SEM) of three independent PCR runs. P-values were calculated using unpaired t-test. The claudin-5 mRNA level was significantly reduced following treatment with Ang-I, VEGF, or TGF-β in a dose-dependent manner. However, the claudin-5 mRNA level was increased following bFGF treatment. E: The effect of VEGF (I ng/ml), Ang-I (I ng/ml), TGF-β (I ng/ml), and bFGF (I ng/ml) on the claudin-5 protein level in PnMECs after a 3-day treatment. F: The bar graph reflects the combined densitometry data from three independent experiments. G: The effect of VEGF, Ang-I, TGF-β, and bFGF on the TEER values across the PnMEC monolayer (mean ± SD, n = 6 in each condition). The TEER values of PnMECs were significantly increased when cultured with bFGF (I ng/ml). In contrast, the TEER values of PnMECs were significantly reduced after treatment with VEGF, Ang-I, or TGF-β. H: The effect of anti-bFGF neutralizing antibody on the claudin-5 induction following treatment with PPCT-CM. The PnMECs were cultured with PPCT-CM or PPCT-CM pretreated with bFGF antibody for 24 h. The level of claudin-5 mRNA in PnMECs was assayed by real-time RT-PCR and expressed as the ratio of the target gene/GAPDH. The claudin-5 mRNA was inhibited by 42% following PPCT-CM pretreated with anti-bFGF antibody in comparison to that treated with only PPCT-CM. I: The change in the level of claudin-5 protein in PnMECs following treatment with anti-bFGF neutralizing antibody using a Western blot analysis. Claudin-5 protein was inhibited after pretreatment with anti-bFGF neutralizing antibody. J: The bar graph reflects the combined densitometry data from three independent experiments. K: The TEER value of PnMECs was significantly reduced by the treatment of PPCT-CM pretreated with anti-bFGF antibody in comparison to that treated with PPCT-CM. NCM, Non-conditioned medium was prepared by the same procedure using DMEM with 20% FBS; PPCT-CM, conditioned medium of peripheral nerve pericytes; PPCT-CM + bFGF antibody, conditioned medium of peripheral nerve pericytes pretreated with bFGF neutralizing antibody.

Discussion

This study successfully established brain and peripheral nerve pericyte cell lines of human origin. Various human immortalized brain endothelial cell lines have been successfully established (Weksler et al., 2005) including ours, and one brain and peripheral nerve endothelial cell line has recently been developed (Sano et al., 2007, 2010). However, neighboring pericytes have long been ignored as barrier-forming cells. Pericytes are an important component of the BBB and BNB and participate in the maintenance of vascular stability (Hellstrom et al., 2001) and in the supply of some cytokines and growth factors to endothelial cells in paracrine manner (Armulik et al., 2005). Therefore, the human BBB- or BNB-derived pericyte cell lines, combined with BBB- or BNB-derived endothelial cells, could shed a novel light on the future studies of BBB and BNB.

Pericyte are morphologically, biochemically, and physiologically heterogeneous and they may have distinctive characteristics in different organs (Armulik et al., 2005). Pericytes are localized at the abluminal side of the microvascular endothelium and are completely enveloped by a basement membrane (Shepro and Morel, 1993). Pericytes increase vascular stability (Hellstrom et al., 2001) and regulate the BBB by secretion of paracrine growth factors (Armulik et al., 2005). However, the molecular mechanisms by which pericytes regulate the barrier function of the BBB are unknown. The BBB comprised endothelial cells, astrocytes, and pericytes of microvascular origin, whereas the BNB comprised endothelial cells and pericytes of endoneurial microvascular origin (Poduslo et al., 1994; Sano et al., 2007). Astrocytes strengthen the barrier function of BMECs via the secretion of soluble factors in the in vitro BBB model (Hori et al., 2004; Kim et al., 2006). The current study also showed that brain pericytes as well as astrocytes have property of increasing barrier integrity of BMECs through claudin-5 up-regulation. Unlike the BBB, the BNB lacks cells that correspond to astrocytes. We therefore hypothesized that peripheral nerve pericytes, which are the only cells composing in endoneurial microvessels other than PnMECs, might strengthen the barrier function of the BNB and play a similar role as that of astrocytes in the BBB. Astrocytes have been reported to regulate the BBB by secretion of paracrine growth factors such as TGF-β, VEGF, and bFGF (Abbott et al., 2006; Kim JH et al., 2006). The current study initially analyzed whether these factors are also secreted by brain and peripheral nerve pericytes. These results demonstrated that brain and peripheral nerve pericytes also expressed several soluble factors such as Ang-1, VEGF, TGF-β, and bFGF, which are secreted by astrocytes in the BBB (Abbott et al., 2006; Fig. 3A,B). In particular, the level of Ang-1, TGF-β, and bFGF in peripheral nerve pericytes was significantly higher than those in brain pericytes and PnMECs and were equivalent to those in astrocytes (Fig. 3C,D,F). Peripheral nerve pericytes secrete these soluble factors and might exert a beneficial effect on endothelial cells maintenance in BNB, thus playing a role similar to that of astrocytes in the BBB.

Pericytes could possibly strengthen the barrier properties of PnMECs by secreting several soluble factors because pericyte-conditioned media significantly increase the TEER value and decrease inulin clearance in PnMECs (Fig. 5B,D,E). It is well known that claudin-5 is a major component of TJs, and the expression level of claudin-5 is important for TJ maintenance in the mature BBB (Nitta et al., 2003). Ohtsuki et al. (2007) reported that exogenous expression of claudin-5 induces barrier properties in cultured rat brain capillary endothelial cells line which do not express claudin-5. Several reports previously demonstrated that the expression of claudin-5 was increased by humoral factors such as adrenomedullin (Honda et al., 2006) and bFGF (Bendfeldt et al., 2007), or reduced by VEGF (Argaw et al., 2009). The current results demonstrated that

claudin-5 expression of PnMECs was not changed after incubation with fibroblasts-conditioned media but significantly increased by treatment with pericyte-conditioned media (Fig. 6A,D,F), thus suggesting that the soluble factors secreted from pericytes affect the barrier property of the endothelial cells in a paracrine manner through the up-regulation of claudin-5 in vivo. Furthermore, this study investigated which soluble factors secreted from pericytes increased claudin-5 expression. These results indicated that the barrier properties of PnMECs in the BNB were augmented by bFGF, and then decreased by VEGF, Ang-1, or TGF-β released from pericytes through change of claudin-5 (Fig. 7A,B,D,E,G–J). Recently, the breakdown of the BNB has been considered to be a key initial step in many autoimmune neuropathies such as Guillain–Barré syndrome and chronic inflammatory demyelinating polyradiculoneuropathy (CIDP) (Lach et al., 1993; Kanda et al., 1994, 2000, 2004). Kanda et al. (2004) reported that the number of claudin-5-positive microvessels in the BNB in cases of CIDP was significantly decreased in comparison to that of patients with non-inflammatory neuropathies. This finding suggests that the modification of the integrity of tight junctions in the BNB may provide novel therapeutic avenues for many autoimmune peripheral neuropathies. The present findings demonstrated that the regulation of these soluble factors secreted from pericytes might have therapeutic potential in repairing and modifying the barrier properties of the BNB in autoimmune peripheral neuropathies.

Next, this study was the first to demonstrate that brain and peripheral nerve pericytes expressed several neurotrophic factors including NGF, GDNF, and BDNF (Fig. 4A,E). The inflammatory mediator TNF-α plays a key role in the pathological processes of Guillain–Barré syndrome and CIDP (Radhakrishnan et al., 2004; Deng et al., 2008; Yang et al., 2008). TNF-α also induces cell-specific damage to Schwann cells in vitro (Boyle et al., 2005) and thus contributes to the development of inflammatory neuropathy. The current study demonstrated that the expression of GDNF (Fig. 4H), BDNF (Fig. 4I), and NGF (Fig. 4J) mRNA in peripheral nerve pericytes was significantly increased after exposure of TNF-α. The physiological role of TNFα in the BNB is unclear, but these results suggested that neurotrophic factors secreted from the peripheral nerve pericytes might have a neuroprotective effect against axonal loss mediated by TNF-α in inflammatory neuropathies such as Guillain–Barré syndrome and CIDP. Interestingly, the GDNF and BDNF protein in peripheral nerve pericytes were significantly higher than those in brain pericytes and astrocytes (Fig. 4F,G). Many studies have shown that astrocytes produce neurotrophic factors such as GDNF and BDNF, which protect against neuronal loss in the central nervous system (Mizuta et al., 2001; Wang et al., 2002). Neurotrophic factors secreted from peripheral nerve pericytes might prevent axonal loss and promote axonal regeneration in the peripheral nervous system (PNS). Although neurotrophic factors such as GDNF, BDNF, and NGF cannot be used for neuroprotection following intravenous administration because these proteins do not cross the BNB, the neurotrophic factors secreted from peripheral nerve pericytes in the endoneurial space may be useful for neuroprotection in the PNS. The modification of these neurotrophic factors released from pericytes may have therapeutic potential for intractable peripheral neuropathies.

In conclusion, BBB or BNB-derived pericytes modify BNB functions through various soluble factors. The regulation of soluble factors secreted from pericytes may thus provide novel therapeutic strategies to modify the BNB functions and promote peripheral nerve regeneration. Further research is thus necessary to elucidate the characteristics of pericytes because knowledge concerning the molecular mechanisms by which pericytes regulate BBB and BNB function under both

physiological and pathological conditions could lead to the development of new therapies for various neurological disorders including diabetic neuropathy and stroke.

Acknowledgments

Literature Cited

Abbott NJ, Rönnbäck L, Hansson E. 2006. Astrocyte–endothelial interactions at the blood–brain barrier. Nat Rev Neurosci 7:41–53.

Argaw AT, Gurfein BT, Zhang Y, Zameer A, John GR. 2009. VEGF-mediated disruption of endothelial CLN-5 promotes blood–brain barrier breakdown. Proc Natl Acad Sci USA 106:1977–1982.

Armulik A, Abramsson A, Betsholtz C. 2005. Endothelial/pericyte interactions. Circ Res 97:512–523.

Bäckman CM, Shan L, Zhang YJ, Hoffer BJ, Leonard S, Troncoso JC, Vonsatel P, Tomac AC. 2006. Gene expression patterns for GDNF and its receptors in the human putamen affected by Parkinson's disease: A real-time PCR study. Mol Cell Endocrinol 27:160–166.

Basciani S, Mariani S, Arizzi M, Ulisse S, Rucci N, Jannini EA, Della Rocca C, Manicone A, Carani C, Spera G, Gnessi L. 2002. Expression of platelet-derived growth factor-A (PDGF-A), PDGF-B, and PDGF receptor-alpha and -beta during human testicular development and disease. J Clin Endocrinol Metab 87:2310–2319.

Bendfeldt K, Radojevic V, Kapfhammer J, Nitsch C. 2007. Basic fibroblast growth factor modulates density of blood vessels and preserves tight junctions in organotypic cortical cultures of mice: A new in vitro model of the blood–brain barrier. J Neurosci 27:3260–3267.

Boyle H, Azari MF, Cheema SS, Petratos S. 2005. TNF-alpha mediates Schwann cell death by upregulating p75NTR expression without sustained activation of NF kappaB. Neurobiol Dis 20:412–427.

Bronzetti E, Artico M, Pompili E, Felici LM, Stringaro A, Bosco S, Magliulo G, Colone M, Arancia G, Vitale M, Fumagalli L. 2006. Neurotrophins and neurotransmitters in human palatine tonsils: An immunohistochemical and RT-PCR analysis. Int J Mol Med 18:49–58.

Brown EB, Campbell RB, Tsuzuki Y, Xu L, Carmeliet P, Fukumura D, Jain RK. 2001. In vivo measurement of gene expression, angiogenesis and physiological function in tumors using multiphoton laser scanning microscopy. Nat Med 7:864–868.

Capetandes A, Gerritsen ME. 1990. Simplified methods for consistent and selective culture of bovine retinal endothelial cells and pericytes. Invest Ophthalmol Vis Sci 31:1738–1744.

Davis S, Aldrich TH, Jones PF, Acheson A, Compton DL, Jain V, Ryan TE, Bruno J, Radziejewski C, Maisonpierre PC, Yancopoulos GD. 1996. Isolation of angiopoietin-1, a ligand for the TIE2 receptor, by secretion-trap expression cloning. Cell 27:1161–1169.

Deng H, Yang X, Jin T, Wu J, Hu LS, Chang M, Sun XJ, Adem A, Winblad B, Zhu J. 2008. The role of IL-12 and TNF-alpha in AIDP and AMAN. Eur J Neurol 15:1100–1105.

Fuchs S, Hermanns MI, Kirkpatrick CJ. 2006. Retention of a differentiated endothelial phenotype by outgrowth endothelial cells isolated from human peripheral blood and expanded in long-term cultures. Cell Tissue Res 326:79–92.

Ghassemifar MR, Eckert JJ, Houghton FD, Picton HM, Leese HJ, Fleming TP. 2003. Gene expression regulating epithelial intercellular junction biogenesis during human blastocyst development in vitro. Mol Hum Reprod 9:245–252.

Giannini C, Dyck PJ. 1995. Basement membrane reduplication and pericyte degeneration precede development of diabetic polyneuropathy and are associated with its severity. Ann Neurol 37:498–504.

Hammes HP. 2005. Pericytes and the pathogenesis of diabetic retinopathy. Horm Metab Res 37:39–43.

Hellstrom M, Gerhardt H, Kalen M, Li X, Eriksson U, Wolburg H, Betsholtz C. 2001. Lack of pericyte leads to endothelial hyperplasia and abnormal vascular morphogenesis. J Cell Biol 30:543–553.

Hirschi KK, Burt JM, Hirschi KD, Dai C. 2003. Gap junction communication mediates transforming growth factor-beta activation and endothelial-induced mural cell differentiation. Circ Res 93:429–437.

Honda M, Nakagawa S, Hayashi K, Kitagawa N, Tsutsumi K, Nagata I, Niwa M. 2006. Adrenomedullin improves the blood–brain barrier function through the expression of claudin-5. Cell Mol Neurobiol 26:109–118.

Hori S, Ohtsuki S, Hosoya K, Nakashima E, Terasaki T. 2004. A pericyte-derived angiopoietin-1 multimeric complex induces occludin gene expression in brain capillary endothelial cells through Tie-2 activation in vitro. J Neurochem 89:503–513.

Hosoya KI, Takashima T, Tetsuka K, Nagura T, Ohtsuki S, Takanaga H, Ueda M, Yanai N, Obinata M, Terasaki T. 2000. mRNA expression and transport characterization of conditionally immortalized rat brain capillary endothelial cell lines; a new in vitro BBB model for drug targeting. J Drug Target 8:357–370.

Huang YQ, Li JJ, Karpatkin S. 2000. Identification of a family of alternatively spliced mRNA species of angiopoietin-1. Blood 15:1993–1999.

Kanda T, Yoshino H, Ariga T, Yamawaki M, Yu RK. 1994. Glycosphingolipid antigens in cultured microvascular bovine brain endothelial cells: Sulfoglucuronosyl paragloboside as a target of monoclonal IgM in demyelinative neuropathy. J Cell Biol 126:235–246.

Kanda T, Iwasaki T, Yamawaki M, Ikeda K. 1997. Isolation and culture of bovine endothelial cells of endoneurial origin. J Neurosci Res 15:769–777.

Kanda T, Yamawaki M, Iwasaki T, Mizusawa H. 2000. Glycosphingolipid antibodies and blood-nerve barrier in autoimmune demyelinating neuropathy. Neurology 54: 1459–1464.

Kanda T, Numata Y, Mizusawa H. 2004. Chronic inflammatory demyelinating polyneuropathy: Decreased claudin-5 and relocated ZO-1. J Neurol Neurosurg Psychiatry 75:765–769.

Kim JH, Kim JH, Park JA, Lee SW, Kim WJ, Yu YS, Kim KW. 2006. Blood–neural barrier: Intercellular communication at glio-vascular interface. J Biochem Mol Biol 39:339–345.

Kondo T, Hosoya K, Hori S, Tomi M, Ohtsuki S, Takanaga H, Nakashima E, Iizasa H, Asashima T, Ueda M, Obinata M, Terasaki T. 2003. Establishment of conditionally immortalized rat retinal pericyte cell lines (TR-rPCT) and their application in a co-culture system using retinal capillary endothelial cell line (TR-iBRB2). Cell Struct Funct 28:145–153.

Lach B, Rippstein P, Atack D, Afar DE, Gregor A. 1993. Immunoelectron microscopic localization of monoclonal IgM antibodies in gammopathy associated with peripheral demyelinating neuropathy. Acta Neuropathol 85:298–307.

Lindahl P, Johansson BR, Leveen P, Betsholtz C. 1997. Pericyte loss and microaneurysm formation in PDGF-B-deficient mice. Science 277:242–245.

Mizuta I, Ohta M, Ohta K, Nishimura M, Mizuta E, Kuno S. 2001. Riluzole stimulates nerve growth factor, brain-derived neurotrophic factor and glial cell line-derived neurotrophic factor synthesis in cultured mouse astrocytes. Neurosci Lett 310:117–120.

Nehls V, Drenckhahn D. 1991. Heterogeneity of microvascular pericytes for smooth muscle type alpha-actin. J Cell Biol 113:147–154.

Niimi H. 2003. Cerebral angiogenesis induced by growth factors: Intravital microscopic studies using models. Clin Hemorheol Microcirc 29:149–156.

Nitta T, Hata M, Gotoh S, Seo Y, Sasaki H, Hashimoto N, Furuse M, Tsukita S. 2003. Size-selective loosening of the blood–brain barrier in claudin-5-deficient mice. J Cell Biol 161:653–660.

Ohtsuki S, Sato S, Yamaguchi H, Kamoi M, Asashima T, Terasaki T. 2007. Exogenous expression of claudin-5 induces barrier properties in cultured rat brain capillary endothelial cells. J Cell Physiol 210:81–86.

Ozerdem U, Grako KA, Dahlin-Huppe K, Monosov E, Stallcup WB. 2001. NG2 proteoglycan is expressed exclusively by mural cells during vascular morphogenesis. Dev Dyn 222:218–227.

Poduslo JF, Curran GL, Berg CT. 1994. Macromolecular permeability across the blood–nerve and blood–brain barriers. Proc Natl Acad Sci USA 91:5705–5709.

Radhakrishnan VV, Sumi MG, Reuben S, Mathai A, Nair MD. 2004. Serum tumour necrosis factor-alpha and soluble tumour necrosis factor receptors levels in patients with Guillain–Barre syndrome. Acta Neurol Scand 109:71–74.

Reinmuth N, Liu W, Jung YD, Ahmad SA, Shaheen RM, Fan F, Bucana CD, McMahon G, Gallick GE, Ellis LM. 2001. Induction of VEGF in perivascular cells defines a potential paracrine mechanism for endothelial cell survival. FASEB J 15:1239–1241.

Said HM, Hagemann C, Staab A, Stojic J, Kühnel S, Vince GH, Flentje M, Roosen K, Vordermark D. 2007. Expression patterns of the hypoxia-related genes osteopontin, CA9, erythropoietin, VEGF and HIF-1 alpha in human glioma in vitro and in vivo. Radiother Oncol 83:398–405.

Sano Y, Shimizu F, Nakayama H, Abe M, Maeda T, Ohtsuki S, Terasaki T, Obinata M, Ueda M, Takahashi R, Kanda T. 2007. Endothelial cells constituting blood–nerve barrier have highly specialized characteristics as barrier-forming cells. Cell Struct Funct 32:139–147.

Sano Y, Shimizu F, Abe M, Maeda T, Kashiwamura Y, Ohtsuki S, Terasaki T, Obinata M, Kajiwara K, Fujii M, Suzuki M, Kanda T. 2010. Establishment of a new conditionally immortalized human brain microvascular endothelial cell line retaining an in vivo blood-brain barrier function. J Cell Physiol 10 (in press).

Sato Y, Rifkin DB. 1989. Inhibition of endothelial cell movement by pericytes and smooth muscle cells: Activation of a latent transforming growth factor-beta 1-like molecule by plasmin during co-culture. J Cell Biol 109:309–315.

Shepro D, Morel NM. 1993. Pericyte physiology. FASEB J 7:1031–1038.

Shimizu F, Sano Y, Maeda T, Abe MA, Nakayama H, Takahashi R, Ueda M, Ohtsuki S, Terasaki T, Obinata M, Kanda T. 2008. Peripheral nerve pericytes originating from the blood–nerve barrier expresses tight junctional molecules and transporters as barrier-forming cells. J Cell Physiol 217:388–399.

Soufla G, Sifakis S, Baritaki S, Zafiropoulos A, Koumantakis E, Spandidos DA. 2005. VEGF, FGF2, TGFB1 and TGFBR1 mRNA expression levels correlate with the malignant transformation of the uterine cervix. Cancer Lett 18:105–118.

Varley CL, Garthwaite MA, Cross W, Hinley J, Trejdosiewicz LK, Southgate J. 2006. PPARgamma-regulated tight junction development during human urothelial cytodifferentiation. J Cell Physiol 208:407–417.

Wang Y, Chang CF, Morales M, Chiang YH, Hoffer J. 2002. Protective effects of glial cell line-derived neurotrophic factor in ischemic brain injury. Ann N Y Acad Sci 962: 423–437.

Weksler BB, Subileau EA, Perrière N, Charneau P, Holloway K, Leveque M, Tricoire-Leignel H, Nicotra A, Bourdoulous S, Turowski P, Male DK, Roux F, Greenwood J, Romero IA, Couraud PO. 2005. Blood–brain barrier-specific properties of a human adult brain endothelial cell line. FASEB J 19:1872–1874.

Yang X, Jin T, Press R, Quezada HC, Fredrikson S, Zhu J. 2008. The expression of TNF-alpha receptors 1 and 2 on peripheral blood mononuclear cells in chronic inflammatory demyelinating polyneuropathy. J Neuroimmunol 200:129–132.

Zhang ZL, Liu ZS, Sun Q. 2006. Expression of angiopoietins, Tie2 and vascular endothelial growth factor in angiogenesis and progression of hepatocellular carcinoma. World J Gastroenterol 12:4241–4245.

ORIGINAL PAPER

Hydrocortisone Enhances the Function of the Blood-Nerve Barrier Through the Up-Regulation of Claudin-5

Yoko Kashiwamura · Yasuteru Sano · Masaaki Abe ·
Fumitaka Shimizu · Hiroyo Haruki · Toshihiko Maeda ·
Motoharu Kawai · Takashi Kanda

Abstract In autoimmune disorders of the peripheral nervous system (PNS), including Guillain–Barré syndrome and chronic inflammatory demyelinating polyradiculoneuropathy, breakdown of the blood-nerve barrier (BNB) has been considered to be a key step in the disease process. Although glucocorticoids (GCs) have been shown to effectively restore the blood–brain barrier (BBB) in some inflammatory central nervous system diseases such as multiple sclerosis, their action against the BNB has not yet been examined. To elucidate the role of GCs on the BNB, we established a novel human immortalized endothelial cell lines derived from the BNB. The established cell line termed "DH-BNBs" expresses two important tight junction proteins, claudin-5 and occludin. Using DH-BNBs, we analyzed how GCs affect BNB function. We herein report that GCs up-regulate the expression of claudin-5 and increase the barrier properties of the BNB. This is the first report which indicates how GCs affect the blood-nerve barrier.

Keywords Blood-nerve barrier · Peripheral nerve microvascular endothelial cells · Tight junction · Claudin-5 · Glucocorticoid

Y. Kashiwamura · Y. Sano · M. Abe · F. Shimizu · H. Haruki ·
T. Maeda · M. Kawai · T. Kanda (✉)
Department of Neurology and Clinical Neuroscience,
Yamaguchi University Graduate School of Medicine,
1-1-1 Minamikogushi, Ube, Yamaguchi 7558505, Japan
e-mail: tkanda@yamaguchi-u.ac.jp

Introduction

The blood-nerve barrier (BNB) is one of the functional barriers sheltering the nervous system from circulating blood [1]. The BNB comprises the endoneurial microvasculature and the innermost layers of the perineurium. Tight junctions (TJs) between adjacent peripheral nerve microvascular endothelial cells (PnMECs) are responsible for BNB function [2, 3]. In the BNB, just like in the blood–brain barrier (BBB), tight junction molecules including occludin, claudin-5, ZO-1, and ZO-2 have an important role in maintaining the BNB function [4]. The breakdown of the BNB has been considered to be an initial key step in many autoimmune disorders of the peripheral nervous system, including Guillain–Barré syndrome, chronic inflammatory demyelinating polyradiculoneuropathy (CIDP), and paraprotemic neuropathy [5–7]. Restoration of the BNB function in these diseases might lead to the development of new therapeutic strategies. Established treatments for CIDP include glucocorticoid (GC) therapy [8, 9], but the detailed mechanisms of its therapeutic action remain unclear. On the other hand, GCs have been shown to effectively restore the BBB in multiple sclerosis (MS) [10] and experimental allergic encephalomyelitis (EAE), a rat model of MS [11]. In addition, some reports indicate that GCs up-regulate TJ proteins and increase the barrier properties of human and mouse brain microvascular endothelial cell lines [12, 13]. However, it remains unclear how GCs modulate the BNB function. In this study, we examined the effects of hydrocortisone (HC) on an endothelial cell line derived from the human BNB. We herein report that HC up-regulates the expression of claudin-5 and increases the barrier properties of the BNB. This is the first study indicating how GCs affect the human blood-nerve barrier.

Springer